

# Heavy Quark Spectroscopy and Matrix Elements: A Lattice Study using the Static Approximation

*UKQCD Collaboration*

**A.K. Ewing<sup>1</sup>, J.M. Flynn, C.T. Sachrajda, N. Stella, H. Wittig<sup>2</sup>**

Physics Department, The University, Southampton SO17 1BJ, UK

**K.C. Bowler, R.D. Kenway, J. Mehegan<sup>3</sup>, D.G. Richards**

Department of Physics & Astronomy, The University of Edinburgh, Edinburgh EH9 3JZ,  
Scotland

**C. Michael**

DAMTP, University of Liverpool, Liverpool L69 3BX, UK

## Abstract

We present results of a lattice analysis of the  $B$  parameter,  $B_B$ , the decay constant  $f_B$ , and several mass splittings using the static approximation. Results were obtained for 60 quenched gauge configurations computed at  $\beta = 6.2$  on a lattice size of  $24^3 \times 48$ . Light quark propagators were calculated using the  $O(a)$ -improved Sheikholeslami-Wohlert action. We find  $B_B^{\text{static}}(m_b) = 0.69 \begin{smallmatrix} +3 \\ -4 \end{smallmatrix} (\text{stat}) \begin{smallmatrix} +2 \\ -1 \end{smallmatrix} (\text{syst})$ , corresponding to  $B_B^{\text{static}} = 1.02 \begin{smallmatrix} +5 \\ -6 \end{smallmatrix} \begin{smallmatrix} +3 \\ -2 \end{smallmatrix}$ , and  $f_B^{\text{static}} = 266 \begin{smallmatrix} +18 \\ -20 \end{smallmatrix} \begin{smallmatrix} +28 \\ -27 \end{smallmatrix} \text{MeV}$ ,  $f_{B_s}^2 B_{B_s} / f_B^2 B_B = 1.34 \begin{smallmatrix} +9 \\ -8 \end{smallmatrix} \begin{smallmatrix} +5 \\ -3 \end{smallmatrix}$ , where a variational fitting technique was used to extract  $f_B^{\text{static}}$ . For the mass splittings we obtain  $M_{B_s} - M_{B_d} = 87 \begin{smallmatrix} +15 \\ -12 \end{smallmatrix} \begin{smallmatrix} +6 \\ -12 \end{smallmatrix} \text{MeV}$ ,  $M_{\Lambda_b} - M_{B_d} = 420 \begin{smallmatrix} +100 \\ -90 \end{smallmatrix} \begin{smallmatrix} +30 \\ -30 \end{smallmatrix} \text{MeV}$  and  $M_{B^*}^2 - M_B^2 = 0.281 \begin{smallmatrix} +15 \\ -16 \end{smallmatrix} \begin{smallmatrix} +40 \\ -37 \end{smallmatrix} \text{GeV}^2$ . We compare different smearing techniques intended to improve the signal/noise ratio. From a detailed assessment of systematic effects we conclude that the main systematic uncertainties are associated with the renormalisation constants relating a lattice matrix element to its continuum counterpart. The dependence of our findings on lattice artefacts is to be investigated in the future.

<sup>1</sup>Present address: Edinburgh Parallel Computing Centre, Edinburgh EH9 3JZ, Scotland

<sup>2</sup>Present address: DESY-IFH, Platanenalle 6, D-15738 Zeuthen, Germany

<sup>3</sup>Present address: Physics Department, University of Wales, Swansea SA2 8PP, UK

# 1 Introduction

Heavy quark systems have attracted considerable interest in recent years. Studying the decays of hadrons containing heavy quarks is important in order to narrow the constraints on the less known elements of the Cabibbo-Kobayashi-Maskawa (CKM) matrix. Precise knowledge of the CKM matrix elements serves to test the consistency of the Standard Model and to detect possible signals of “new physics”. Theoretical tools for dealing with heavy quark systems, such as the Heavy Quark Effective Theory (HQET) [1, 2, 3], have been developed and are being successfully applied in the analysis and interpretation of experimental data. However, theoretical estimates of form factors, decay constants and mixing parameters are subject to uncertainties due to strong interaction effects whose nature is intrinsically non-perturbative on typical hadronic scales. Lattice simulations of QCD are designed to provide a non-perturbative treatment of hadronic processes and have already made important contributions to the study of the spectroscopy and decays of hadrons in both the light and heavy quark sector [4]. For systems involving heavy quarks, most notably the  $b$  quark, the rôle of lattice simulations is two-fold: firstly, to make predictions for yet unmeasured quantities such as the decay constant of the  $B$  meson,  $f_B$ , or the masses of baryons containing  $b$  quarks; secondly, to test the validity of other theoretical methods such as large mass expansions or the HQET.

One problem that is encountered in current simulations of heavy quark systems is the fact that typical values of the inverse lattice spacing lie in the range  $2 - 3.5$  GeV which is well below the  $b$  mass. There are several methods for dealing with this problem, one of which was proposed by Eichten [5] in which the heavy quark propagator is expanded in inverse powers of the heavy quark mass. The so-called static approximation is the leading term in this expansion, for which the  $b$  quark is infinitely heavy. One may also hope to compute some of the higher-order corrections to the static limit, although the presence of power divergences presents theoretical and practical complications [6].

Another method for lattice studies of heavy quark systems is to use propagating heavy quarks. At present, these simulations are carried out for quark masses around the charm quark mass, and the results obtained in this fashion must be extrapolated to the mass of the  $b$  quark. Clearly, this method depends crucially on controlling the effects of non-zero lattice spacing (“lattice artefacts”) at the heavy masses used in the simulation. In general, the influence of lattice artefacts on quantities involving propagating quarks can be reduced by considering “improved” actions as suggested by Symanzik [7] and detailed further by the authors of [8] and [9]. For heavy-light decay constants, improvement has been successfully applied to quark masses in the region of that of the charm quark [10, 11]. Furthermore, the data from the static approximation, obtained at infinite quark mass, serve to guide the extrapolation of results obtained using propagating heavy quarks to the mass of the  $b$ .

In this paper we report on our results for  $f_B$ , the  $B$  parameter  $B_B$  describing  $B^0 - \overline{B}^0$  mixing and mass splittings involving the  $B$  and  $B^*$  mesons as well as the  $\Lambda_b$ . The results are obtained using the static approximation for the heavy quark, whereas the  $O(a)$ -improved Sheikholeslami-Wohlert action [8, 9] is used for the light quarks. In many ways this study is intended as a continuation and extension of earlier simulations. For example, we are able to study the effects of  $O(a)$ -improvement on various quantities, among them the  $B^* - B$  mass splitting, which is believed to be sensitive to discretisation errors. Furthermore, this splitting arises only at next-to-leading order in the large mass expansion and serves therefore as a measure of higher-order corrections to the static limit.

We now list our main results. For the  $B$  parameter at scale  $m_b$  in the static approximation we obtain

$$B_{B_d}^{\text{static}}(m_b) = 0.69 \begin{smallmatrix} +3 \\ -4 \end{smallmatrix} (\text{stat}) \begin{smallmatrix} +2 \\ -1 \end{smallmatrix} (\text{syst}), \quad (1)$$

which corresponds to a value of the renormalisation-group-invariant  $B$  parameter of

$$B_{B_d}^{\text{static}} = 1.02 \begin{smallmatrix} +5 \\ -6 \end{smallmatrix} (\text{stat}) \begin{smallmatrix} +3 \\ -2 \end{smallmatrix} (\text{syst}). \quad (2)$$

The decay constant  $f_B^{\text{static}}$  is found to be

$$f_{B_d}^{\text{static}} = 266 \begin{smallmatrix} +18 \\ -20 \end{smallmatrix} (\text{stat}) \begin{smallmatrix} +28 \\ -27 \end{smallmatrix} (\text{syst}) \text{ MeV}. \quad (3)$$

From the chiral behaviour of  $B_B^{\text{static}}$  and  $f_B^{\text{static}}$  we extract

$$\frac{f_{B_s}^2 B_{B_s}}{f_{B_d}^2 B_{B_d}} = 1.34 \begin{smallmatrix} +9 \\ -8 \end{smallmatrix} (\text{stat}) \begin{smallmatrix} +5 \\ -3 \end{smallmatrix} (\text{syst}). \quad (4)$$

Finally, for the mass splittings we obtain

$$M_{B_s} - M_{B_d} = 87 \begin{smallmatrix} +15 \\ -12 \end{smallmatrix} (\text{stat}) \begin{smallmatrix} +6 \\ -12 \end{smallmatrix} (\text{syst}) \text{ MeV} \quad (5)$$

$$M_{\Lambda_b} - M_{B_d} = 420 \begin{smallmatrix} +100 \\ -90 \end{smallmatrix} (\text{stat}) \begin{smallmatrix} +30 \\ -30 \end{smallmatrix} (\text{syst}) \text{ MeV} \quad (6)$$

$$M_{B^*}^2 - M_B^2 = 0.281 \begin{smallmatrix} +15 \\ -16 \end{smallmatrix} (\text{stat}) \begin{smallmatrix} +40 \\ -37 \end{smallmatrix} (\text{syst}) \text{ GeV}^2. \quad (7)$$

Here, the systematic error on dimensionful quantities is dominated by uncertainties in the lattice scale, whereas systematic errors on dimensionless quantities arise from the spread of values using alternative fitting procedures. There is an additional uncertainty in the estimate of the  $B$  parameter, which arises from the perturbative matching between full QCD and the lattice theory in the static approximation. We estimate this uncertainty to be as large as 15–20%, as will be discussed later.

Our estimate for the  $B^* - B$  hyperfine splitting in eq. (7) is much smaller than the experimental value of  $0.488(6) \text{ GeV}^2$  (as is also the case with Wilson fermions [13]). The implications of this result are discussed in more detail in section 4.3. Here we only wish to state that the relevant matching factor for the  $B^* - B$  splitting is also subject to significant uncertainties.

It is beyond the scope of this paper to investigate the dependence of our results on the lattice spacing  $a$ . Here we wish to stress that we seek to reduce these effects considerably by employing an  $O(a)$ -improved fermionic action, leaving an extrapolation to the continuum limit to future studies.

The paper is organised as follows. In section 2 we describe the details of our simulation and analysis. Section 3 contains our results for  $B_B^{\text{static}}$  and  $f_B^{\text{static}}$ . The splittings  $B_s - B_d$ ,  $B^* - B$  and  $\Lambda_b - B$  are discussed in section 4. Finally, section 5 contains a summary and our conclusions.

## 2 The Simulation

Our results are based on 60 SU(3) gauge configurations in the quenched approximation, calculated on a lattice of size  $24^3 \times 48$  at  $\beta = 6.2$ . The configurations were generated using the hybrid over-relaxed algorithm described in [14].

Light quark propagators were computed at three values of the hopping parameter  $\kappa_l$ , namely  $\kappa_l = 0.14144$ ,  $0.14226$  and  $0.14262$ , using the Sheikholeslami-Wohlert (SW) action [8]

$$S_F^{SW} = S_F^W - i \frac{\kappa_l}{2} \sum_{x,\mu,\nu} \bar{q}(x) F_{\mu\nu}(x) \sigma_{\mu\nu} q(x), \quad (8)$$

where  $S_F^W$  is the standard Wilson action and  $F_{\mu\nu}$  is a lattice definition of the field strength tensor [14].

The chosen  $\kappa_l$  values are in the region of the strange quark, whose mass, as determined from the mass ratio  $m_K^2/m_\rho^2$ , corresponds to  $\kappa_s = 0.1419(1)$ , while the chiral limit of massless quarks is reached at  $\kappa_{\text{crit}} = 0.14315(2)$  [15].

The leading term in the expansion of the heavy quark propagator is given by

$$S_Q(\vec{x}, t; \vec{0}, 0) = \left\{ \Theta(t) e^{-m_Q t} \frac{1 + \gamma^4}{2} + \Theta(-t) e^{m_Q t} \frac{1 - \gamma^4}{2} \right\} \delta^{(3)}(\vec{x}) \mathcal{P}_{\vec{0}}(t, 0), \quad (9)$$

where  $\mathcal{P}_{\vec{0}}(t, 0)$  is the product of links from  $(\vec{0}, t)$  to the origin, for example for  $t > 0$ ,

$$\mathcal{P}_{\vec{0}}(t, 0) = U_4^\dagger(\vec{0}, t - 1) U_4^\dagger(\vec{0}, t - 2) \cdots U_4^\dagger(\vec{0}, 0). \quad (10)$$

The static quark propagator, eq. (9), and the light quark propagators were combined to compute correlation functions for the relevant quantities in this paper.

In order to obtain  $O(a)$ -improved matrix elements for heavy-light bilinears using the static approximation, it is sufficient to carry out the improvement prescription in the light quark sector only [27]. Therefore we describe the light quark using the SW action and consider operators in which only the light quark field  $q(x)$  has been “rotated” [9, 10], i.e.

$$O_\Gamma = b^\dagger(x) \Gamma (1 - \frac{1}{2} \gamma \cdot \vec{D}) q(x). \quad (11)$$

Here,  $b(x)$  denotes the heavy quark spinor in the static approximation, and  $\Gamma$  is some Dirac matrix.

It is useful to use extended (or “smeared”) interpolating operators in order to isolate the ground state in correlation functions efficiently. This is of particular importance in the static approximation where calculations using purely local operators are known to fail [16]. In this study we compare different smearing techniques which can be broadly divided into gauge-invariant and gauge-dependent methods, the latter being performed on gauge configurations transformed to the Coulomb gauge.

For gauge-invariant smearing we use the Jacobi smearing algorithm described in [17]. The smeared field at timeslice  $t$ ,  $q^S(\vec{x}, t)$  is defined by

$$q^S(\vec{x}, t) \equiv \sum_{\vec{x}'} J(x, x') q(\vec{x}', t) \quad (12)$$

where

$$J(x, x') = \sum_{n=0}^N \kappa_S \Delta^n(x, x'), \quad (13)$$

and  $\Delta$  is the gauge-invariant discretised version of the three-dimensional Laplace operator. The parameter  $\kappa_S$  and the number of iterations  $N$  can be used to control the smearing radius. Here, we quote our results for  $\kappa_S = 0.25$  and  $N = 140$ , which corresponds to a r.m.s. smearing radius of  $r_0 = 6.4$  [10]. The same values were used in our previous study of  $f_B^{\text{static}}$ , obtained on a subset of 20 of our 60 gauge configurations [10].

In order to study smearing methods in a fixed gauge, the configurations were transformed to the Coulomb gauge using the algorithms described in [18, 19]. The lattice analog of the continuum Coulomb gauge condition,  $\partial_i A_i(x) = 0$ , is

$$\theta(x) = \text{Tr}(D(x)D^\dagger(x)) = 0 \quad (14)$$

where

$$D(x) = \sum_i \left( U_i(x) + U_i^\dagger(x-i) - \text{h.c.} \right)_{\text{traceless}} \quad (15)$$

with the index  $i$  signifying spatial components only. At each iteration of the gauge fixing procedure the average value of  $\theta$  was calculated,  $\langle \theta \rangle = \sum_x \theta(x)/V$ , where  $V$  is the total lattice volume. For each gauge configuration the gauge was fixed to a precision  $\langle \theta \rangle \sim 10^{-4}$ .

Defining the smeared quark field  $q^S(\vec{x}, t)$  via

$$q^S(\vec{x}, t) \equiv \sum_{\vec{x}'} f(\vec{x}, \vec{x}') q(\vec{x}', t) \quad (16)$$

we considered the following smearing functions  $f(\vec{x}, \vec{x}')$  for smearing radius  $r_0$ :

$$\text{Exponential : } f(\vec{x}, \vec{x}') = \exp \{ -|\vec{x} - \vec{x}'|/r_0 \} \quad (17)$$

$$\text{Gaussian : } f(\vec{x}, \vec{x}') = \exp \left\{ -|\vec{x} - \vec{x}'|^2 / r_0^2 \right\} \quad (18)$$

$$\text{Cube : } f(\vec{x}, \vec{x}') = \prod_{i=1}^3 \Theta(r_0 - |x_i - x'_i|) \quad (19)$$

$$\text{Double Cube : } f(\vec{x}, \vec{x}') = \prod_{i=1}^3 \left( 1 - \frac{|x_i - x'_i|}{2r_0} \right) \Theta(2r_0 - |x_i - x'_i|). \quad (20)$$

Following the analysis in ref. [20], where a variety of smearing radii was studied, we chose  $r_0 = 5$  in all cases.

Our 60 gauge configurations and the light quark propagators were computed on the 64-node Meiko i860 Computing Surface at Edinburgh. The transformation to the Coulomb gauge was performed on the Cray Y-MP/8 at the Daresbury Rutherford Appleton Laboratory. Smeared propagators using the gauge-invariant Jacobi algorithm were calculated on a Thinking Machines CM-200 at the University of Edinburgh. All other smearing types and the relevant correlators were computed on a variety of DEC ALPHA machines.

Statistical errors are estimated from a bootstrap procedure [21], which involves the creation of 200 bootstrap samples from our set of 60 configurations. Correlators are fitted for each sample by minimising  $\chi^2$ , taking correlations among different timeslices into account. The quoted statistical errors are obtained from the central 68% of the corresponding bootstrap distribution [14].

In order to convert our values for decay constants and mass splittings into physical units we need an estimate of the inverse lattice spacing in GeV. In this study we take

$$a^{-1} = 2.9 \pm 0.2 \text{ GeV}, \quad (21)$$

thus deviating slightly from some of our earlier papers where we quoted 2.7 GeV as the central value [10, 14, 15]. The error in eq. (21) is large enough to encompass all our estimates for  $a^{-1}$  from quantities such as  $m_\rho$ ,  $f_\pi$ ,  $m_N$ , the string tension  $\sqrt{K}$  and the hadronic scale  $R_0$  discussed in [22]. The shift was partly motivated by a recent study using newly generated UKQCD data [23]: using the quantity  $R_0$  we found  $a^{-1} = 2.95^{+7}_{-11} \text{ GeV}$ . Also, a non-perturbative determination of the renormalisation constant of the axial current resulted in a value of  $Z_A = 1.04$  [24] which is larger by about 8% than the perturbative value which we had used previously. Thus the scale as estimated from  $f_\pi$  decreases to around 3.1 GeV which enables us to significantly reduce the upper uncertainty on our final value of  $a^{-1}$  [GeV].

### 3 Decay Constants and Mixing Parameters

In this section we present the results for  $f_B^{\text{static}}$  and  $B_B^{\text{static}}$ . We begin by listing the various operators in the lattice effective theory and discussing the relevant renormalisation factors.

Here, we wish to emphasise that all our matching and scaling factors are consistently defined at leading order in the strong coupling constant. The 2- and 3-point correlators are defined before the results are discussed. We close the section with a discussion of the phenomenological implications of our findings.

### 3.1 Lattice Operators and Renormalisation

In the continuum full theory, the pseudoscalar decay constant of the  $B$  meson is defined through the matrix element of the axial current:

$$\langle 0 | A_\mu(0) | B(\vec{p}) \rangle = i p_\mu f_B, \quad A_\mu(x) = \bar{b}(x) \gamma_\mu \gamma_5 q(x). \quad (22)$$

The  $\Delta B = 2$  four-fermi operator  $O_L$  which gives rise to  $B^0 - \overline{B}^0$  mixing is given by

$$O_L = \left( \bar{b} \gamma_\mu (1 - \gamma_5) q \right) \left( \bar{b} \gamma_\mu (1 - \gamma_5) q \right). \quad (23)$$

This operator enters the effective Hamiltonian describing  $B^0 - \overline{B}^0$  mixing whose amplitude is usually expressed in terms of the  $B$  parameter, which is the ratio of the operator matrix element to its value in the vacuum insertion approximation

$$B_B(\mu) = \frac{\langle \overline{B}^0 | O_L(\mu) | B^0 \rangle}{\frac{8}{3} f_B^2 M_B^2}, \quad (24)$$

where  $\mu$  is a renormalisation scale. We have adopted a convention in which  $f_\pi = 132$  MeV. The scale dependence of  $B_B(\mu)$  can be removed by multiplication with a factor derived from the anomalous dimension of the operator  $O_L$ . At one-loop order, one can define a renormalisation-group-invariant  $B$  parameter by

$$B_B = \alpha_s(\mu)^{-2/\beta_0} B_B(\mu), \quad (25)$$

where  $\beta_0 = 11 - 2n_f/3$ . The strong coupling constant appearing in the above expression is usually defined in the  $\overline{\text{MS}}$  scheme. We will use the one-loop expression for  $B_B$  below, since it is consistent with our matching between lattice and continuum results, which is performed at order  $\alpha_s$ . Alternative matching procedures and higher-order scalings of  $B_B(\mu)$  can always be incorporated by suitably replacing our matching and scaling factors.

In order to get estimates for the matrix elements of the axial current and of the four-fermi operator  $O_L$  in the continuum, these operators need to be matched to the relevant lattice operators in the static effective theory. The matching of operators in the static approximation is usually performed as a two-step process, in which one first matches the operators in the effective theory on the lattice to those in the continuum effective theory. In the second step, one then matches the continuum effective theory to the operator in full QCD.

For the axial current, this two-step matching process was considered for Wilson fermions to one-loop order in [25, 26] and extended to the  $O(a)$ -improved case in [27] and [28].

At  $\mu = a^{-1}$  the renormalisation factor between full QCD and the lattice effective theory at order  $\alpha_s$  for the SW action is

$$Z_A^{\text{static}} = 1 + \frac{\alpha_s^c(a^{-1})}{4\pi} \left\{ 2 \ln(a^2 m_b^2) - 2 \right\} - 15.02 \frac{\alpha_s^{\text{latt}}(a^{-1})}{3\pi}. \quad (26)$$

In order to evaluate  $Z_A^{\text{static}}$  numerically for  $m_b = 5 \text{ GeV}$ , we define the strong coupling constant for  $n_f$  active quark flavours at leading order in the continuum by

$$\alpha_s^c(\mu) \equiv \frac{2\pi}{\beta_0 \ln(\mu/\Lambda_{\overline{\text{MS}}}^{(n_f)})} \quad (27)$$

where  $\beta_0 = 11 - \frac{2}{3}n_f$ , and we take  $n_f = 4$ ,  $\Lambda_{\overline{\text{MS}}}^{(4)} = 200 \text{ MeV}$ ,  $\mu = a^{-1} = 2.9 \text{ GeV}$ . Thus, despite the fact that our results for matrix elements of lattice operators are obtained in the quenched approximation, we use the relevant number of active quark flavours at the respective renormalisation scale when matching the continuum effective theory to full QCD. This concept implies that we abandon the quenched approximation once we have obtained the matrix elements in the continuum effective theory after the first matching step. Of course, all our results are still subject to a systematic error due to quenching, which is, however, hard to quantify unless precision data from dynamical simulations become available.

For the matching step between the effective theories in the continuum and on the lattice we take the “boosted” value for the gauge coupling [29, 30]

$$\alpha_s^{\text{latt}}(a^{-1}) = \frac{6}{4\pi \beta u_0^4} \quad (28)$$

where  $u_0$  is a measure of the average link variable, for which we take  $u_0 = (8\kappa_{\text{crit}})^{-1}$  with  $\kappa_{\text{crit}} = 0.14315(2)$  [15]. With these definitions, we find

$$Z_A^{\text{static}} = 0.78. \quad (29)$$

This is very close to the value of  $Z_A^{\text{static}} = 0.79$  quoted in our previous study [10], and also to  $Z_A^{\text{static}} = 0.81$  used in a simulation by the APE collaboration [36] employing the SW action for light quarks at  $\beta = 6.2$ .

In the case of the four-fermi operator the situation is more complicated due to operator mixing. When relating the full continuum theory to the continuum effective theory, it is useful to introduce

$$O_S = \left( \bar{b}(1 - \gamma_5) q \right) \left( \bar{b}(1 - \gamma_5) q \right). \quad (30)$$

This operator is generated at order  $\alpha_s$  in the continuum owing to the mass of the heavy quark [31]. The one-loop matching factors between the continuum full theory at scale  $m_b$



and the continuum effective theory at scale  $\mu < m_b$  are given by<sup>4</sup>

$$O_L^{\text{full}}(m_b) = \left\{ 1 + \frac{g^2}{16\pi^2} [4 \ln(m_b^2/\mu^2) + C_L] \right\} O_L^{\text{eff}}(\mu) + \frac{g^2}{16\pi^2} C_S O_S^{\text{eff}}(\mu) \quad (31)$$

with  $C_L = -14$  and  $C_S = -8$  [31].

In the matching step between the continuum effective and the lattice effective theories, two additional operators are generated due to the explicit chiral symmetry breaking induced by the Wilson term

$$O_R = (\bar{b} \gamma_\mu (1 + \gamma_5) q) (\bar{b} \gamma_\mu (1 + \gamma_5) q) \quad (32)$$

$$\begin{aligned} O_N &= (\bar{b} \gamma_\mu (1 - \gamma_5) q) (\bar{b} \gamma_\mu (1 + \gamma_5) q) \\ &+ (\bar{b} \gamma_\mu (1 + \gamma_5) q) (\bar{b} \gamma_\mu (1 - \gamma_5) q) \\ &+ 2 (\bar{b} (1 - \gamma_5) q) (\bar{b} (1 + \gamma_5) q) \\ &+ 2 (\bar{b} (1 + \gamma_5) q) (\bar{b} (1 - \gamma_5) q). \end{aligned} \quad (33)$$

For the  $O(a)$ -improved SW action, the full one-loop matching for the four-fermi operator  $O_L^{\text{eff}}$  to the lattice effective theory at scale  $\mu = a^{-1}$  is given by

$$\begin{aligned} O_L^{\text{eff}}(a^{-1}) &= \left\{ 1 + \frac{\alpha_s^{\text{latt}}(a^{-1})}{4\pi} [D_L + D_L^I] \right\} O_L^{\text{latt}} \\ &+ \frac{\alpha_s^{\text{latt}}(a^{-1})}{4\pi} [D_R + D_R^I] O_R^{\text{latt}} + \frac{\alpha_s^{\text{latt}}(a^{-1})}{4\pi} [D_N + D_N^I] O_N^{\text{latt}} \end{aligned} \quad (34)$$

The coefficients  $D_L$ ,  $D_R$ ,  $D_N$  were calculated in [31], whereas those for the SW action,  $D_L^I$ ,  $D_R^I$ ,  $D_N^I$  are listed in [27]. A subtle point to note is that the coefficient  $D_L$  is quoted as  $D_L = -65.5$  in refs. [31, 27]. In [26] it was stated, however, that the reduced value of the quark self-energy should be used if the static-light meson propagator is being fitted to the usual exponential. Using the reduced value  $e^{(R)}$  in the formula for  $D_L$  yields a value of  $D_L = -38.9$ , and hence results in a much smaller correction to  $O_L^{\text{eff}}$  in the matching step between the lattice effective and the continuum effective theory. In the following we quote numerical values for all relevant renormalisation constants using the reduced value of the quark self-energy. It should be added that the expression for  $Z_A^{\text{static}}$  in eq. (26) is also based on the reduced value  $e^{(R)}$ , and thus our procedure to extract the  $B$  parameter from a suitable ratio of matrix elements in the static theory is entirely consistent.

Expanding the various matching factors to order  $\alpha_s$ , we arrive at the following expression for the matching of the operator  $O_L^{\text{full}}(m_b)$  to the operators in the lattice effective theory:

$$O_L^{\text{full}}(m_b) = \left\{ 1 + \frac{\alpha_s^c(a^{-1})}{4\pi} [4 \ln(a^2 m_b^2) - 14] - 22.06 \frac{\alpha_s^{\text{latt}}(a^{-1})}{4\pi} \right\} O_L^{\text{latt}}$$

---

<sup>4</sup>Note that in refs. [31, 27] the operator  $O_L^{\text{full}}$  is obtained at the scale  $\mu = a^{-1} < m_b$ . This requires the factor 4 multiplying  $\ln(m_b^2/\mu^2)$  to be replaced by a factor 6, which is the difference of the anomalous dimensions in the continuum full and continuum effective theories.

$$- 4.19 \frac{\alpha_s^{\text{latt}}(a^{-1})}{4\pi} O_R^{\text{latt}} - 13.96 \frac{\alpha_s^{\text{latt}}(a^{-1})}{4\pi} O_N^{\text{latt}} - 2 \frac{\alpha_s^c(a^{-1})}{\pi} O_S^{\text{latt}} \quad (35)$$

$$\equiv Z_L O_L^{\text{latt}} + Z_R O_R^{\text{latt}} + Z_N O_N^{\text{latt}} + Z_S O_S^{\text{latt}}. \quad (36)$$

It is this expression which we will use from now on to convert our lattice results into an estimate of the  $B$  parameter.

Using our numerical values for the coupling constants  $\alpha_s(a^{-1})$  and  $\alpha_s^{\text{latt}}(a^{-1})$  we find

$$Z_L = 0.55, \quad Z_R = -0.04, \quad Z_N = -0.15, \quad Z_S = -0.18. \quad (37)$$

As was already mentioned in [31], the correction to the matrix element of  $O_L^{\text{latt}}$  is rather large, thus calling the applicability of one-loop perturbative matching into question. In fact, if the matching is performed by first computing  $O_L^{\text{eff}}(a^{-1})$  according to eq. (34), and then inserting the result into eq. (31), we observe that our estimate for  $B_B$  increases by 20 %. This way of matching includes some part of the  $O(\alpha_s^2)$  contributions to the renormalisation factors, and hence it serves to estimate the influence of higher loop corrections in the matching procedure.

In reference [32] the two-loop anomalous dimensions of the axial current and the four-fermi operator were calculated for the effective theory in the continuum. Including this result into the matching step between  $O_L^{\text{full}}(m_b)$  and  $O_L^{\text{eff}}(\mu)$  in eq. (31) changes the final result only by 1–2 %. Therefore we conclude that the bulk of the uncertainty arises from the matching step between the continuum effective and lattice effective theories, and also from the large factor of  $C_L = -14$  in eq. (31). An entirely non-perturbative determination of the renormalisation constants relating  $O_L^{\text{eff}}$  to the different lattice operators, as outlined in [33], is highly desirable in order to clarify this important issue, which is of equal importance in the case of  $Z_A^{\text{static}}$ , as will be illustrated later.

### 3.2 Correlators for 2- and 3-point Functions

In order to extract the pseudoscalar decay constant we consider the correlation function of the time-component of the improved static-light axial current

$$\sum_{\vec{x}} \langle A_4(\vec{x}, t) A_4^\dagger(\vec{0}, 0) \rangle \xrightarrow{t \gg 0} \frac{f_B^2 M_B}{2} e^{-M_B t}. \quad (38)$$

In practice, using particular combinations of the smeared ( $S$ ) and local ( $L$ ) axial current, we compute correlation functions defined by

$$C^{SS}(t) = \sum_{\vec{x}} \langle 0 | A_4^S(\vec{x}, t) A_4^{\dagger S}(\vec{0}, 0) | 0 \rangle \xrightarrow{t \gg 0} (Z^S)^2 e^{-E t} \quad (39)$$

$$C^{LS}(t) = \sum_{\vec{x}} \langle 0 | A_4^L(\vec{x}, t) A_4^{\dagger S}(\vec{0}, 0) | 0 \rangle \xrightarrow{t \gg 0} Z^S Z^L e^{-E t}, \quad (40)$$

$$C^{SL}(t) = \sum_{\vec{x}} \langle 0 | A_4^S(\vec{x}, t) A_4^{\dagger L}(\vec{0}, 0) | 0 \rangle \xrightarrow{t \gg 0} Z^S Z^L e^{-E t}, \quad (41)$$

where  $E$  is the unphysical difference between the mass of the meson and the bare mass of the heavy quark.

The pseudoscalar decay constant  $f_B^{\text{static}}$  is related to  $Z^L$  via

$$f_B^{\text{static}} = Z^L \sqrt{\frac{2}{M_B}} Z_A^{\text{static}}, \quad (42)$$

where  $M_B$  is the mass of the  $B$  meson.

$Z^L$  and thus  $f_B^{\text{static}}$  is extracted from  $C^{SS}(t)$  and  $C^{LS}(t)$  as follows: by fitting  $C^{SS}(t)$  to the functional form given in eq. (39) we obtain  $Z^S$  and  $E$ . At sufficiently large times the ratio  $C^{LS}(t)/C^{SS}(t) \rightarrow Z^L/Z^S$ , so that  $Z^L$  can be determined. As was observed earlier [34, 35, 10], using the correlation function  $C^{LS}(t)$  in which the operator at the source is smeared yields much better statistics than the corresponding correlator  $C^{SL}(t)$  for which the smearing is performed at the sink.

Alternative methods, discussed in [36], include a direct fit of  $C^{LS}(t)$  in order to extract  $Z^L Z^S$  which can then be combined with the ratio  $Z^L/Z^S$  to compute  $Z^L$ . However, this method requires the ground state to be unambiguously isolated, which is more difficult for  $C^{LS}(t)$ , since the plateau in the effective mass plot is approached from below.

A more direct method, which does not involve any fitting and was also advocated in [36], is to consider the ratio

$$R_{Z^L}(t_1, t_2) = \frac{C^{LS}(t_1) C^{LS}(t_2)}{C^{SS}(t_1 + t_2)} \rightarrow (Z^L)^2. \quad (43)$$

Here, however, one needs a reliable signal for fairly large times  $t_1 + t_2$ . Since the authors of [36] accumulated 220 configurations they were able to apply this method successfully, which turned out to be consistent with the other ones. In view of our smaller statistical sample, we did not use the ratio  $R_{Z^L}(t_1, t_2)$  to extract  $f_B^{\text{static}}$ .

In order to determine the  $B$  parameter we computed the relevant 3-point correlator using the following expression

$$K_i^{SS}(t_1, t_2) \equiv \sum_{\vec{x}_1, \vec{x}_2} \langle 0 | T \{ A^{\dagger S}(\vec{x}_1, -t_1) O_i^{\text{latt}}(0) A^{\dagger S}(\vec{x}_2, t_2) \} | 0 \rangle \\ \xrightarrow{t_1, t_2 \gg 0} \frac{(Z^S)^2}{2 M_B} e^{-E(t_1 + t_2)} \langle \overline{B^0} | O_i^{\text{latt}} | B^0 \rangle, \quad (44)$$

where  $i = L, R, S, N$  labels the four operators in the lattice effective theory, and  $A^S(\vec{x}, t)$  is the smeared axial current. In order to cancel the contributions from  $Z^S$  and the exponentials in eq. (44) we consider suitable ratios of  $K_i^{SS}(t_1, t_2)$  and the 2-point correlator  $C^{SL}(t)$ , i.e. with the local operators always at the origin and the smearing performed at the same timeslices in both the numerator and denominator.

Using the definition of  $B_B(\mu)$  in the continuum theory eq. (24), and defining the ratio

$R_i^{SS}(t_1, t_2)$  in the lattice effective theory as

$$R_i^{SS}(t_1, t_2) = \frac{K_i^{SS}(t_1, t_2)}{\frac{8}{3} C^{SL}(t_1) C^{SL}(t_2)} \quad (45)$$

then, provided  $t_1, t_2 \gg 0$ , the  $B$  parameter at scale  $m_b$  is obtained from

$$\sum_i Z_i (Z_A^{\text{static}})^{-2} R_i^{SS}(t_1, t_2) \xrightarrow{t_1, t_2 \gg 0} B_B(m_b), \quad i = L, R, S, N \quad (46)$$

with the  $Z_i$ 's given in eq. (37).

In the computation of the ratio  $R_i^{SS}(t_1, t_2)$  on a periodic lattice we expect a signal for the correlator describing  $B^0 - \overline{B}^0$  mixing for  $t_1$  and  $t_2$  on opposite halves of the lattice [37], i.e.

$$\begin{aligned} 0 < t_1 < T/2, \\ T/2 < t_2 < T, \end{aligned} \quad (47)$$

where  $T = 48$  is the length of our lattice in the time direction. In order to exploit time-reversal symmetry and thus to enhance the signal for the correlator, we compute the ratio  $R_i^{SS}(t_1, t_2)$  from

$$R_i^{SS}(t_1, t_2) = \frac{[K_i^{SS}(t_1, t_2) + K_i^{SS}(T - t_1, T - t_2)]}{\frac{4}{3} [C^{SL}(t_1) + C^{SL}(T - t_1)] [C^{SL}(t_2) + C^{SL}(T - t_2)]} \quad (48)$$

The correlators were calculated for timeslices  $2 \leq t_1 \leq 12$  and  $36 \leq t_2 \leq 46$ , which includes the entire region where one expects their asymptotic behaviour.

### 3.3 Results for $B_B^{\text{static}}$

In this subsection we present the results for the  $B$  parameter  $B_B^{\text{static}}$  using different smearing methods. For gauge-fixed configurations the four types of smearing defined in eqs. (17) – (20) were used, i.e. exponential (EXP), gaussian (GAU), cube (CUB) and double cube smearing (DCB). The results from the gauge-invariant Jacobi smearing algorithm are labelled (INV).

We begin by describing the two methods we used to extract  $B_B^{\text{static}}(\mu)$  at renormalisation scale  $\mu = m_b$  from the ratios  $R_i^{SS}(t_1, t_2), i = L, R, S, N$ .

**Method (a):** The four ratios  $R_i^{SS}(t_1, t_2)$  are fitted individually to their asymptotic values  $R_i$ . The  $B$  parameter is then obtained through

$$B_B^{\text{static}}(m_b) = \sum_i Z_i (Z_A^{\text{static}})^{-2} R_i, \quad (49)$$

with the factors  $Z_i$  given in eq. (37).

**Method (b):** Using the four ratios  $R_i^{SS}(t_1, t_2)$ , we define the  $B$  parameter  $\tilde{B}_B^{\text{static}}(m_b; t_1, t_2)$  for each set of timeslices  $(t_1, t_2)$

$$\tilde{B}_B^{\text{static}}(m_b; t_1, t_2) = \sum_i Z_i (Z_A^{\text{static}})^{-2} R_i^{SS}(t_1, t_2), \quad (50)$$

and fit  $\tilde{B}_B^{\text{static}}(m_b; t_1, t_2)$  to a constant in suitably chosen intervals of  $(t_1, t_2)$ .

The plateaux in the ratios  $R_i^{SS}(t_1, t_2)$  can most conveniently be identified by fixing  $t_1$  at  $t_1 = t_f < T/2$ , and studying  $R_i^{SS}(t_1, t_2)$  as a function of  $t_2$  only.

In order to illustrate method (a) we show in Figure 1 the plateaux for the four ratios  $R_i^{SS}(t_f, t_2)$  for  $t_f = 3$ , using Jacobi smearing at  $\kappa_l = 0.14144$ . It is seen that a good signal is obtained for the four lattice operators, on the backward half of the lattice as expected.

In Figure 2 we show the signal for  $\tilde{B}_B^{\text{static}}(m_b; t_f, t_2)$  obtained using method (b) for both cube and Jacobi smearing. Despite the slightly shorter plateau for cube smearing which is also observed for all other smearing types in Coulomb gauge, the signal obtained in this fashion is also very clear.

As one goes to smaller quark masses, the signals become noisier but are still of good quality, and the plateaux can easily be identified. For the other smearing types computed in the Coulomb gauge the picture is similar, and therefore we do not show the plots corresponding to Figs. 1 and 2. In general,  $\tilde{B}_B^{\text{static}}(m_b; t_f, t_2)$  and the ratios  $R_i^{SS}$  show slightly larger statistical errors when Jacobi smearing is used, but, apart from that, the different smearing types give very similar results.

We have also studied the behaviour of the plateaux for different values of  $t_f$ . Using a larger value, e.g.  $t_f = 4$  leads to bigger errors in the ratios  $R_i^{SS}(t_f, t_2)$  and  $\tilde{B}_B^{\text{static}}(m_b; t_f, t_2)$ , and the plateaux are shifted to smaller values in  $t_2$ . On the other hand, using  $t_f = 2$  gives smaller statistical errors, but the plateaux are less flat which leads to higher  $\chi^2/\text{dof}$  when fitting the ratios to a constant. We emphasise that the ratios are statistically compatible for  $t_f = 2, 3, 4$  for all smearing types considered. Hence, for our best estimates, using either method (a) or (b), we perform a simultaneous fit to the plateaux observed for  $t_f = 3, 4$ . The results obtained by combining the plateaux for  $t_f = 2, 3, 4$  are quoted as a systematic error on our final value for  $B_B^{\text{static}}$ .

The values for  $B_B^{\text{static}}(m_b)$  extracted using methods (a) and (b) are entirely consistent. We have a slight preference for method (a): it gives better plateaux and offers more flexibility in the fitting procedure by ensuring that each of the four contributions are fitted in a region where the respective asymptotic behaviour has been reached. In the following therefore we base all our estimates on method (a). Correlations between different timeslices were taken into account in each fit. We did not attempt a simultaneous fit allowing for cross-correlations between different operators and timeslices, as systematic effects among the four operators

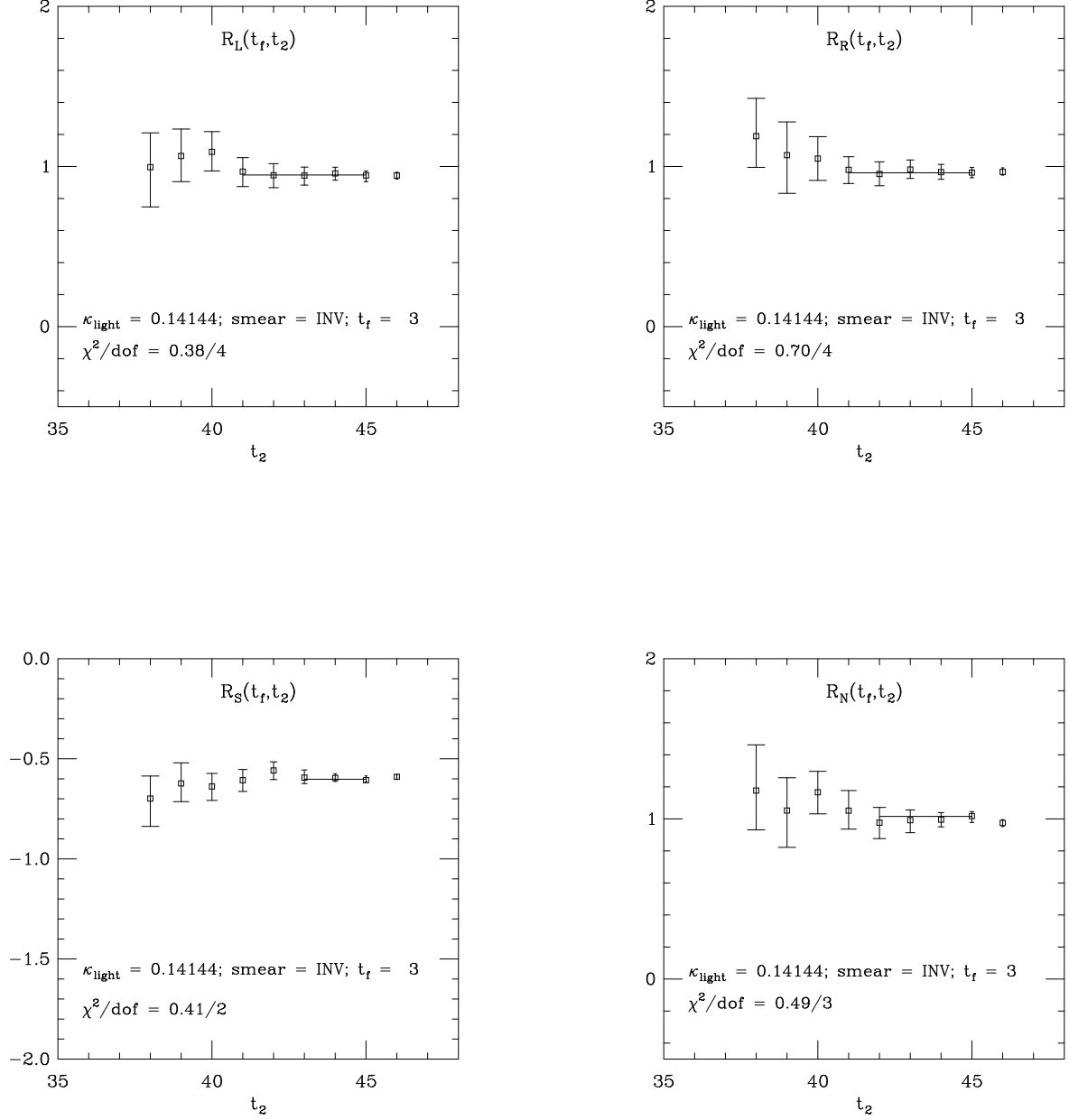


Figure 1: The ratios  $R_L^{SS}(t_f, t_2)$ ,  $R_R^{SS}(t_f, t_2)$ ,  $R_S^{SS}(t_f, t_2)$  and  $R_N^{SS}(t_f, t_2)$  for  $t_f = 3$  and  $\kappa_l = 0.14144$  using Jacobi smearing. The solid lines represent the fits over the respective time interval.

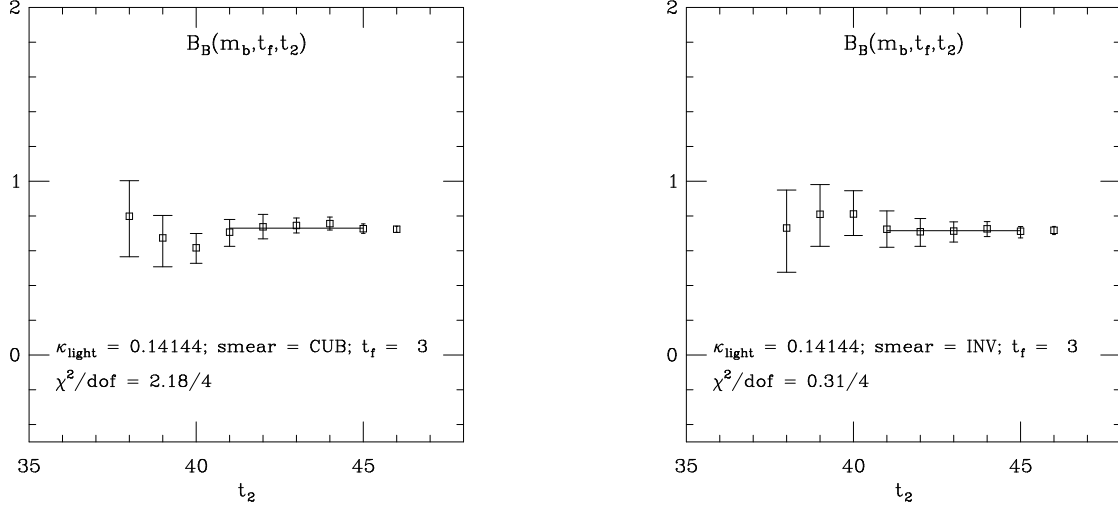


Figure 2: The quantity  $\tilde{B}_B^{\text{static}}(m_b; t_f, t_2)$  defined in eq. (50) for cube smearing (left) and Jacobi smearing (right) at  $\kappa_l = 0.14144$  and  $t_f = 3$ .

could well be different. As was noted in ref. [38], this could lead to an amplification of systematic errors in the fitted values.

In Table 3.3 we show the results from fitting the ratios  $R_i^{SS}(t_1, t_2)$  to a constant for the three light hopping parameters and for all smearing types considered, and also list  $\chi^2/\text{dof}$  and the value for  $B_B^{\text{static}}(m_b)$  after renormalisation according to eq. (49). A remarkable feature is the consistency of the results among all smearing types considered, which we take as evidence that the asymptotic behaviour has been reached.

The values for the ratios  $R_L$ ,  $R_R$  and  $R_N$  of the operators which mix due to the explicit chiral symmetry breaking induced by the Wilson term, are close to one, which is in accordance with the expectation from the vacuum insertion approximation.

One notices only a weak dependence of the four ratios and of  $B_B^{\text{static}}(m_b)$  on the light quark mass. In fact, the results for  $B_B^{\text{static}}(m_b)$  are compatible with a completely flat chiral behaviour within statistical errors as was already noted in [12]. Assuming a linear dependence on the mass of the light quark, we can now extrapolate our results for  $B_B^{\text{static}}(m_b)$  to the chiral limit at  $\kappa_{\text{crit}} = 0.14315(2)$  or to the mass of the strange quark which, according to [15], is found at  $\kappa_s = 0.1419(1)$ . Figure 3 shows the chiral extrapolations of  $B_B^{\text{static}}(m_b)$  for cube and Jacobi smearing from both correlated and uncorrelated fits. Although the measured values appear to be almost perfectly linear as a function of the quark mass, the correlated extrapolation misses the points at smaller quark masses which might signal the use of a bad

$\kappa_l$	smearing				
0.14144	EXP	GAU	CUB	DCB	INV
$R_L$	$0.96^{+2}_{-2}$	$0.97^{+2}_{-2}$	$0.95^{+3}_{-2}$	$0.96^{+2}_{-2}$	$0.94^{+2}_{-3}$
$\chi^2/\text{dof}$	4.72/5	4.81/5	6.13/5	4.89/5	0.86/5
$R_R$	$0.97^{+3}_{-2}$	$0.97^{+2}_{-2}$	$0.96^{+3}_{-2}$	$0.97^{+2}_{-2}$	$0.96^{+3}_{-3}$
$\chi^2/\text{dof}$	8.54/7	7.90/6	9.60/6	7.85/6	2.26/5
$R_S$	$-0.61^{+1}_{-1}$	$-0.61^{+1}_{-1}$	$-0.61^{+1}_{-2}$	$-0.61^{+1}_{-1}$	$-0.60^{+2}_{-1}$
$\chi^2/\text{dof}$	2.29/4	2.48/4	2.68/4	2.46/4	0.92/4
$R_N$	$1.01^{+3}_{-3}$	$1.00^{+3}_{-3}$	$1.01^{+3}_{-4}$	$1.01^{+3}_{-3}$	$1.02^{+3}_{-4}$
$\chi^2/\text{dof}$	4.54/5	5.52/5	4.67/5	5.05/5	1.95/5
$B_B^{\text{static}}(m_b)$	$0.72^{+2}_{-2}$	$0.74^{+2}_{-2}$	$0.72^{+3}_{-2}$	$0.73^{+2}_{-2}$	$0.71^{+2}_{-3}$
0.14226	EXP	GAU	CUB	DCB	INV
$R_L$	$0.94^{+2}_{-2}$	$0.96^{+2}_{-2}$	$0.94^{+3}_{-3}$	$0.95^{+2}_{-2}$	$0.93^{+3}_{-4}$
$\chi^2/\text{dof}$	4.00/5	4.31/5	5.74/5	4.29/5	0.79/5
$R_R$	$0.99^{+3}_{-2}$	$0.97^{+2}_{-2}$	$0.97^{+3}_{-3}$	$0.98^{+2}_{-2}$	$0.98^{+4}_{-3}$
$\chi^2/\text{dof}$	8.48/7	9.38/6	10.92/6	8.92/6	2.56/5
$R_S$	$-0.61^{+1}_{-2}$	$-0.61^{+1}_{-1}$	$-0.60^{+1}_{-2}$	$-0.61^{+1}_{-2}$	$-0.59^{+2}_{-1}$
$\chi^2/\text{dof}$	1.87/4	2.00/4	2.03/4	1.97/4	1.19/4
$R_N$	$1.02^{+3}_{-3}$	$1.00^{+2}_{-3}$	$1.02^{+3}_{-4}$	$1.01^{+3}_{-3}$	$1.02^{+3}_{-4}$
$\chi^2/\text{dof}$	3.01/5	4.62/5	3.45/5	3.79/5	1.85/5
$B_B^{\text{static}}(m_b)$	$0.71^{+3}_{-2}$	$0.73^{+2}_{-2}$	$0.71^{+3}_{-3}$	$0.72^{+2}_{-2}$	$0.69^{+3}_{-4}$
0.14262	EXP	GAU	CUB	DCB	INV
$R_L$	$0.92^{+3}_{-3}$	$0.95^{+2}_{-2}$	$0.93^{+3}_{-3}$	$0.94^{+3}_{-2}$	$0.92^{+3}_{-4}$
$\chi^2/\text{dof}$	3.05/5	3.51/5	4.80/5	3.33/5	0.60/5
$R_R$	$1.02^{+3}_{-3}$	$0.98^{+2}_{-2}$	$0.98^{+3}_{-3}$	$0.99^{+2}_{-3}$	$1.00^{+4}_{-3}$
$\chi^2/\text{dof}$	8.03/7	10.90/6	11.70/6	9.95/6	2.82/5
$R_S$	$-0.61^{+2}_{-2}$	$-0.61^{+1}_{-1}$	$-0.60^{+2}_{-2}$	$-0.61^{+1}_{-2}$	$-0.59^{+2}_{-2}$
$\chi^2/\text{dof}$	2.54/4	2.01/4	1.88/4	2.21/4	1.47/4
$R_N$	$1.01^{+2}_{-4}$	$1.01^{+2}_{-3}$	$1.02^{+3}_{-4}$	$1.01^{+3}_{-3}$	$1.01^{+3}_{-4}$
$\chi^2/\text{dof}$	2.23/5	4.01/5	2.71/5	3.04/5	2.25/5
$B_B^{\text{static}}(m_b)$	$0.69^{+3}_{-3}$	$0.72^{+3}_{-2}$	$0.70^{+3}_{-3}$	$0.72^{+3}_{-2}$	$0.69^{+3}_{-5}$

Table 1: Results for the fits to the ratios of the four lattice operators using method (a).



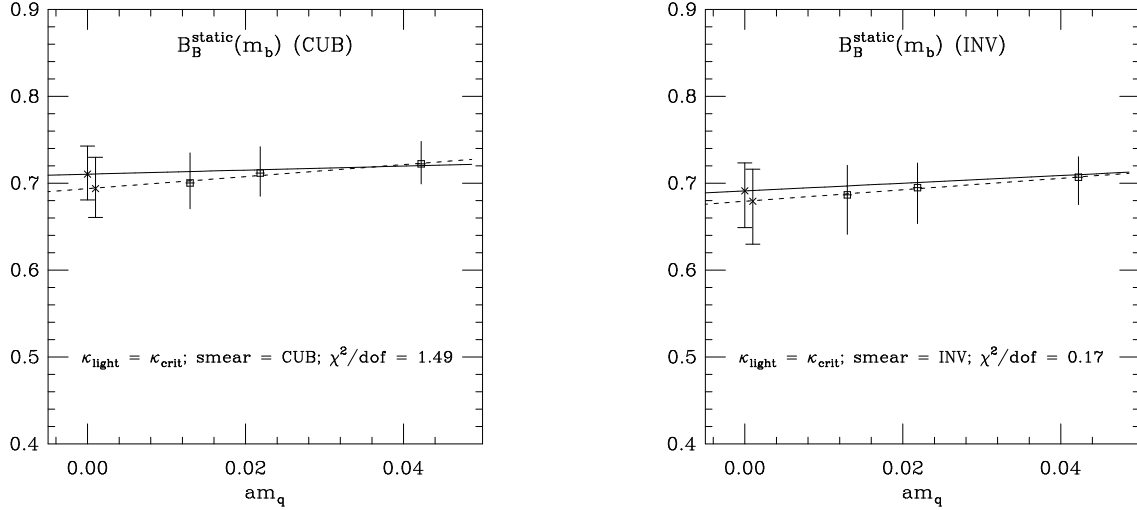


Figure 3: Chiral extrapolations of  $B_B^{\text{static}}(m_b)$  for cube smearing (left) and gauge-invariant smearing (right). The solid lines denote a correlated chiral extrapolation, whereas the uncorrelated fits are denoted by the dashed line. The extrapolated values from both procedures are shifted slightly in  $am_q$ .

fitting function. This results in a higher value for  $B_B^{\text{static}}(m_b)$  in the chiral limit than that from the uncorrelated fit. The values for  $B_B^{\text{static}}(m_b)$  from the two extrapolations agree well within errors, but except for Jacobi smearing the correlated fits have fairly large  $\chi^2/\text{dof}$ .

We quote our best estimates for  $B_B^{\text{static}}(m_b)$  at  $\kappa_{\text{crit}}$  and  $\kappa_s$  from the correlated chiral extrapolation. The measured values at the three light hopping parameters are shown with the extrapolated results in Table 3.3. In the following we will quote our best estimate from Jacobi smearing, which gave the cleanest chiral extrapolation.

Combining the spread of values obtained from using different smearing functions and fitting intervals, extracting  $B_B^{\text{static}}(m_b)$  using method (b), and from performing uncorrelated fits into an estimate of systematic errors, we find

$$B_{B_d}(m_b) = 0.69^{+3}_{-4}(\text{stat})^{+2}_{-1}(\text{syst}) \quad (51)$$

$$B_{B_s}(m_b) = 0.71^{+3}_{-3}(\text{stat})^{+1}_{-1}(\text{syst}). \quad (52)$$

At leading order, the renormalisation-group-invariant  $B$  parameter  $B_B^{\text{static}}$  is obtained from  $B_B^{\text{static}}(m_b)$  according to eq. (25) for  $n_f = 5$  active quark flavours via

$$B_B^{\text{static}} = \alpha_s(m_b)^{-6/23} B_B^{\text{static}}(m_b) \simeq 1.476 B_B^{\text{static}}(m_b), \quad (53)$$

$\kappa_l$	EXP	GAU	CUB	DCB	INV
0.14144	0.72 $^{+2}_{-2}$	0.74 $^{+2}_{-2}$	0.72 $^{+3}_{-2}$	0.73 $^{+2}_{-2}$	0.71 $^{+2}_{-3}$
0.14226	0.71 $^{+3}_{-2}$	0.73 $^{+2}_{-2}$	0.71 $^{+3}_{-3}$	0.72 $^{+2}_{-2}$	0.69 $^{+3}_{-4}$
0.14262	0.69 $^{+3}_{-3}$	0.72 $^{+3}_{-2}$	0.70 $^{+3}_{-3}$	0.72 $^{+3}_{-2}$	0.69 $^{+3}_{-5}$
$\kappa_{\text{crit}}$	0.70 $^{+3}_{-3}$	0.73 $^{+3}_{-3}$	0.71 $^{+3}_{-3}$	0.72 $^{+3}_{-2}$	0.69 $^{+3}_{-4}$
$\kappa_s$	0.72 $^{+3}_{-2}$	0.73 $^{+2}_{-2}$	0.72 $^{+3}_{-2}$	0.73 $^{+2}_{-2}$	0.71 $^{+3}_{-3}$
$\chi^2/\text{dof}$	2.56/1	1.91/1	1.49/1	1.85/1	0.19/1

Table 2: Correlated chiral extrapolations of  $B_B^{\text{static}}(m_b)$  to  $\kappa_{\text{crit}}$  and  $\kappa_s$  for all smearing types considered.

where we have taken  $\Lambda_{\overline{\text{MS}}}^{(5)} = 130 \text{ MeV}$  in the expression for  $\alpha_s$ , eq. (27), in accordance with the relation between  $\Lambda_{\overline{\text{MS}}}^{(4)}$  and  $\Lambda_{\overline{\text{MS}}}^{(5)}$  given in [39]. We obtain

$$B_{B_d} = 1.02 \text{ }^{+5}_{-6}(\text{stat}) \text{ }^{+3}_{-2}(\text{syst}) \quad (54)$$

$$B_{B_s} = 1.04 \text{ }^{+4}_{-5}(\text{stat}) \text{ }^{+2}_{-1}(\text{syst}). \quad (55)$$

Within our errors we conclude that in the static approximation the matrix element of the four-fermi  $\Delta B = 2$  operator is indeed consistent with one. However, if the matching of matrix elements between full QCD and the lattice effective theory is performed using eqs. (31) and (34), rather than eq. (35), as was discussed in subsection 3.1, the above values change to  $B_{B_d} = 1.19 \text{ }^{+5}_{-6} \text{ }^{+3}_{-2}$  and  $B_{B_s} = 1.21 \text{ }^{+4}_{-5} \text{ }^{+2}_{-1}$ , respectively. Therefore we conclude that our best estimates in eqs. (54) and (55) are subject to a further 20 % uncertainty arising from higher-order contributions to the renormalisation constants. A method demonstrating how to determine these factors non-perturbatively was discussed in [33].

In previous lattice calculations of the  $B$  parameter using the static approximation [5, 12], the matching factors  $Z_i$ ,  $i = L, R, N, S$  were still unknown. The authors of [12] obtained results for the ratio  $R_L$ , which are consistent with our findings (see Table 3.3).

In two other simulations [40, 41], propagating heavy Wilson quarks with masses around  $m_{\text{charm}}$  were used to compute the  $B$  parameter. In ref. [40] results were quoted for the quantities  $B_{LL}^{\text{latt}}$  and  $B_{LR}^{\text{latt}}$ , which correspond to our definitions of  $R_L, R_R$ . Extrapolating their results to the mass of the  $B$  meson, the authors of [40] find  $B_{LL}^{\text{latt}} = 1.01 \pm 0.06 \pm 0.18$ ,  $B_{LR}^{\text{latt}} = 1.16 \pm 0.01 \pm 0.11$ , which again is in agreement with our results for  $R_L, R_R$  in Table 3.3. Performing a similar extrapolation in the heavy quark mass, the authors of [41] compute the renormalisation-group-invariant  $B$  parameter as  $B_{B_d} = 1.16 \pm 0.07$ , which is not incompatible with our result at infinite quark mass, given the additional perturbative

uncertainty in  $B_{B_d}$  and  $B_{B_s}$ . We wish to stress that the calculation of the  $B$  parameter should be repeated with propagating heavy quarks using an  $O(a)$ -improved action in order to study  $1/m_Q$  corrections to our result by analysing the mass dependence of  $B_B$ .

### 3.4 Results for $f_B^{\text{static}}$

In this subsection we present our results for  $f_B^{\text{static}}$  extracted using different smearing functions. As outlined in subsection 3.2, our best estimates are obtained by first fitting  $C^{SS}(t)$  to extract the binding energy  $E$  and  $(Z^S)^2$ . The value of  $Z^S$  is then combined with the ratio  $Z^L/Z^S$  obtained from a fit to  $C^{LS}(t)/C^{SS}(t)$ , in order to extract  $Z^L$ .

It has been suggested that this method of determining  $Z^L$  and subsequently  $f_B^{\text{static}}$  potentially suffers from an incomplete isolation of the ground state [42]. Failure to extract the ground state results in higher values for the binding energy and consequently in higher values for  $Z^S$  and hence  $Z^L$ . Therefore the authors of [42] followed a variational approach, based on smearing functions obtained using a relativistic quark model. The variational approach was also used by the authors of [43] who constructed the complete set of smearing functions allowed by the cubic group for a given lattice size.

In a recent study by the APE Collaboration [44] a number of checks for the isolation of the ground state without using the variational approach were presented. As will be shown later in this subsection, our results for  $f_B^{\text{static}}$  are entirely consistent with those in [44].

Here, for the gauge-fixed configurations, in addition to exponential smearing (EXP), we also used a radially-excited exponential smearing function (EXP2S) defined by

$$f(\vec{x}, \vec{x}') = |\vec{x} - \vec{x}'| \exp \{ -|\vec{x} - \vec{x}'|/r_0 \} \quad (56)$$

which is expected to have a considerable overlap with higher states. We then employed a variational approach to estimate the size of possible contamination of the correlators from the first excited state. Our values for  $E$ ,  $Z^S$  and  $Z^L$  from 2-state fits were then compared to the results obtained from the other smearing functions using the procedure outlined in subsection 3.2.

Following ref. [45], we constructed a matrix correlator  $C_{ij}^{SS}(t)$  using the EXP and EXP2S smearing types as a  $2 \times 2$  variational basis and determined the eigenvalues and -vectors of the generalised eigenvalue equation

$$C_{ij}^{SS}(t+1) v_j^{(\alpha)} = \lambda_\alpha(t+1, t) C_{ij}^{SS}(t) v_j^{(\alpha)}. \quad (57)$$

For sufficiently large times  $t$ , the eigenvalues  $\lambda_\alpha$  approach the eigenvalues of the transfer matrix, and therefore

$$\lambda_1(t+1, t) \xrightarrow{t \gg 0} e^{-E} \quad (58)$$

$$\lambda_2(t+1, t) \xrightarrow{t \gg 0} e^{-E^*} \quad (59)$$

where  $E, E^*$  are the binding energies of the ground and first excited states respectively. Hence the quantity

$$\delta_{\text{eff}}(t) \equiv \log \frac{\lambda_1(t+1, t)}{\lambda_2(t+1, t)} \quad (60)$$

approaches the energy difference  $\Delta E = E^* - E$  for sufficiently large  $t$ . In Table 3.4 we show the values of  $\delta_{\text{eff}}(t)$  as a function of  $t$  for all three values of  $\kappa_l$ . It appears that  $\delta_{\text{eff}}(t)$  shows a plateau already for times around  $t = 2$ . Therefore we fix  $\Delta E$  to be  $\delta_{\text{eff}}(t = 2)$  and perform a constrained 3-parameter fit of the correlation function  $C^{SS}(t)$ ,  $S = \text{EXP}$  according to

$$C^{SS}(t) \simeq (Z^S)^2 e^{-Et} \left\{ 1 + \frac{(Z^{S*})^2}{(Z^S)^2} e^{-\Delta Et} \right\} \quad (61)$$

where  $Z^{S*}$  is the amplitude of the first excited state. It is this fitting form which we will from now on call a 2-state fit, whereas the usual 1-state fit is defined in eq. (39). It is possible in principle to use the eigenvector  $v_j^{(1)}$  corresponding to the eigenvalue  $\lambda_1$  to project the matrix correlator onto the approximate ground state. However, the resulting correlation function does not differ appreciably from the one computed using the usual 1S exponential smearing function, and therefore we did not pursue this possibility further.

	$\delta_{\text{eff}}(t)$		
$t$	0.14144	0.14226	0.14262
2	$0.23 \begin{smallmatrix} +5 \\ -5 \end{smallmatrix}$	$0.23 \begin{smallmatrix} +5 \\ -4 \end{smallmatrix}$	$0.23 \begin{smallmatrix} +5 \\ -3 \end{smallmatrix}$
3	$0.23 \begin{smallmatrix} +6 \\ -5 \end{smallmatrix}$	$0.24 \begin{smallmatrix} +6 \\ -4 \end{smallmatrix}$	$0.24 \begin{smallmatrix} +6 \\ -4 \end{smallmatrix}$
4	$0.21 \begin{smallmatrix} +9 \\ -7 \end{smallmatrix}$	$0.23 \begin{smallmatrix} +9 \\ -7 \end{smallmatrix}$	$0.24 \begin{smallmatrix} +9 \\ -7 \end{smallmatrix}$

Table 3: The effective energy difference for the first three computed timeslices at all values of the hopping parameter of the light quark.

In order to compare the results from the 1- and 2-state fits, we follow ref. [42] and plot the results for  $E$  and  $Z^L$  obtained from 1-state fits to both EXP and EXP2S correlators over a time window  $t_{\min}, t_{\max}$  as a function of  $\exp\{-\Delta E t_{\min}\}$ . Keeping the length of the fitting window fixed at  $t_{\max} - t_{\min} = 6$  and increasing  $t_{\min}$  allows one to extrapolate the results from the 1-state fits to  $t = \infty$ . Therefore, as  $t_{\min}$  is increased, we expect that the results from 1-state fits converge to the value obtained from the 2-state fit performed over a large interval in  $t$ .

In fact, as Figure 4 shows, the results from the 1-state fit for the 1S exponential smearing function (EXP) are in agreement with the 2-state fit already for  $t_{\min} = 2$ . Furthermore, the

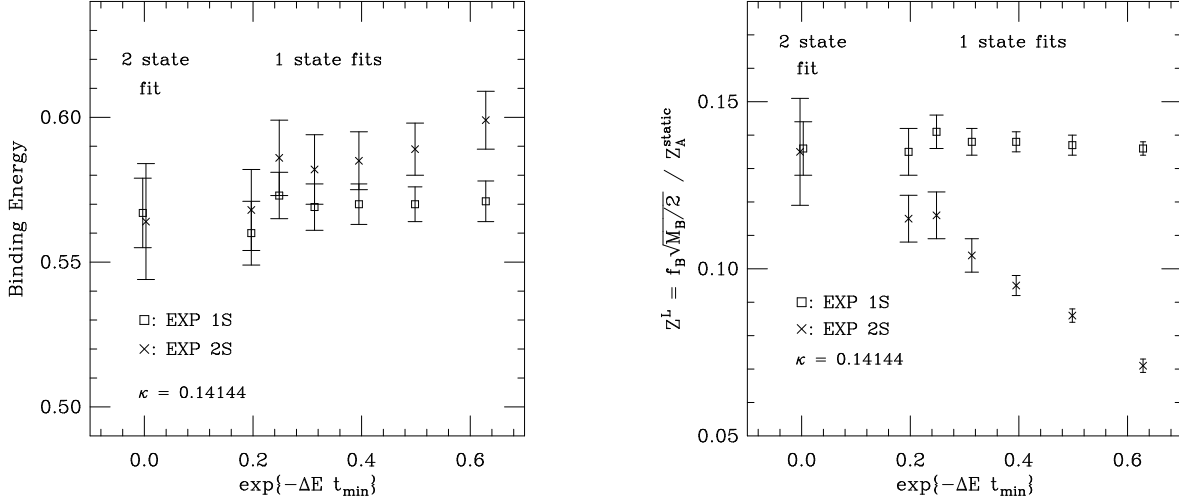


Figure 4: Values for the binding energy and  $Z^L$  obtained from 2-state fits compared to 1-state fits performed using a “sliding” window  $t_{\min}$ ,  $t_{\max}$ , as a function of  $\exp\{-\Delta E t_{\min}\}$  for exponential smearing functions at  $\kappa_l = 0.14144$ .

results for the 1-state fits using the 2S exponential smearing function, which is supposed to have a poorer overlap onto the ground state, show indeed the expected stronger dependence on  $t_{\min}$ . We conclude that the fitting form eq. (39) applied to the 1S exponentially smeared correlator is able to isolate the ground state correctly, provided the fitting interval is chosen suitably. Thus the 2-state fit merely serves to confirm the result obtained using the 1-state fit. This observation is further strengthened by comparing the fitted values for  $E$ ,  $(Z^S)^2$  and  $Z^L$  for 1- and 2-state fits. The comparison is shown in Table 3.4 for one value of the light hopping parameter.

The CUB and DCB smearing types are more problematic. Here, the plateaux for the  $C^{SS}(t)$  correlators only start around  $t_{\min} = 6, 7$  compared to  $t_{\min} = 4, 5$  for EXP and INV smearing. The results from 1-state fits for the binding energy, however, are quite consistent with the results from EXP and INV, whereas the values for  $Z^L$  are higher. Using  $\Delta E$  determined from EXP smearing in a 2-state fit of the CUB and DCB correlators results in lower values for  $Z^L$  but with a significant increase of the statistical errors. Single cube smearing (CUB) is particularly bad in this respect. One may suspect that the cube size was not tuned correctly in order to optimise the overlap of the operators. However, in [46] it was shown that sizes of  $r_0 = 4$  and 6 gave substantially worse results than  $r_0 = 5$ .

At any rate, the values for  $Z^L$  from all smearing methods differ by at most one to two standard deviations, which is remarkably consistent, given the very different smearing functions

	EXP		INV
	2-state fit	1-state fit	1-state fit
$E$	$0.567^{+11}_{-13}$	$0.569^{+6}_{-6}$	$0.570^{+6}_{-4}$
$(Z^S)^2$	$0.0113^{+12}_{-14}$	$0.0115^{+4}_{-4}$	$(1.20^{+5}_{-6}) \cdot 10^3$
$(Z^{S*})^2/(Z^S)^2$	$0.05^{+20}_{-15}$		
$t_{\min}, t_{\max}$	2, 11	4, 11	5, 11
$\chi^2/\text{dof}$	3.2/7	3.1/6	0.6/5
$Z^L$	$0.136^{+7}_{-9}$	$0.137^{+3}_{-3}$	$0.138^{+3}_{-3}$

Table 4: The binding energy  $E$ ,  $(Z^S)^2$ , the ratio  $(Z^{S*})^2/(Z^S)^2$  between the first excited state and the ground state, and the final result for  $Z^L$  for 1- and 2-state fits for exponential, and 1-state fits for gauge-invariant smearing at  $\kappa_l = 0.14144$ . Also shown are the respective fitting ranges.

employed to enhance the signal of the ground state.

We have thus established consistency between the results from 1-state and 2-state exponentially smeared correlators, plus consistency among exponential and gauge-invariant smearing. We have also checked the stability of our results when directly fitting the correlator  $C^{LS}(t)$  and computing  $Z^L$  from  $\sqrt{R(t) \times Z^L Z^S}$ . As was reported in [46], results from exponential and gauge-invariant smearing are stable under the variation of the fitting procedure, whereas CUB and DCB smearing exhibit greater sensitivity to the method and fitting ranges employed.

The results for the binding energy  $E$  and  $Z^L$  for all values of  $\kappa_l$  are shown in Table 3.4. Also shown are the extrapolated values at  $\kappa_{\text{crit}}$  and  $\kappa_s$  which were obtained assuming a linear dependence of  $E$  and  $Z^L$  on the light quark mass.

In the following we will take the results from the 2-state fits of the exponentially smeared correlators as our best estimate. Thereby we ensure that the more conservative choice of a larger statistical error encompasses all systematic variations in the final numbers from using gauge-invariant smearing and/or different fitting procedures. Thus, we do not quote an additional systematic error, and our final answer for  $Z^L$  at  $\kappa_{\text{crit}}$  is

$$Z^L = 0.112^{+8}_{-8} \quad (62)$$

which is in excellent agreement with ref. [36] in which  $Z^L = 0.111(6)$  is quoted. At the common value of  $\kappa_l = 0.14144$  in this work and ref. [36], the values of  $E$  and  $Z^L$  are consistent. Therefore we conclude that the small discrepancy between the binding energy obtained by APE and that in our earlier work [10] based on a subset of 20 configurations, has been

	EXP		CUB	DCB	INV
$E$	1-state	2-state	1-state	1-state	1-state
$t_{\min}, t_{\max}$	4 – 11	2 – 11	7 – 11	7 – 11	5 – 11
0.14144	0.569 $^{+6}_{-6}$	0.567 $^{+11}_{-13}$	0.566 $^{+8}_{-10}$	0.572 $^{+7}_{-7}$	0.570 $^{+6}_{-4}$
0.14226	0.550 $^{+7}_{-6}$	0.548 $^{+13}_{-14}$	0.547 $^{+10}_{-11}$	0.553 $^{+9}_{-7}$	0.550 $^{+6}_{-5}$
0.14262	0.544 $^{+9}_{-7}$	0.542 $^{+13}_{-17}$	0.539 $^{+11}_{-12}$	0.546 $^{+9}_{-8}$	0.543 $^{+7}_{-6}$
$\kappa_{\text{crit}}$	0.528 $^{+10}_{-6}$	0.526 $^{+15}_{-15}$	0.527 $^{+11}_{-12}$	0.522 $^{+12}_{-10}$	0.528 $^{+7}_{-5}$
$\kappa_s$	0.557 $^{+8}_{-6}$	0.556 $^{+13}_{-12}$	0.555 $^{+9}_{-10}$	0.552 $^{+10}_{-8}$	0.557 $^{+8}_{-5}$
$Z^L$	1-state	2-state	1-state	1-state	1-state
0.14144	0.137 $^{+3}_{-3}$	0.136 $^{+7}_{-9}$	0.147 $^{+6}_{-6}$	0.146 $^{+6}_{-5}$	0.138 $^{+3}_{-3}$
0.14226	0.126 $^{+3}_{-3}$	0.125 $^{+6}_{-8}$	0.134 $^{+6}_{-6}$	0.133 $^{+6}_{-6}$	0.126 $^{+3}_{-3}$
0.14262	0.122 $^{+3}_{-3}$	0.121 $^{+7}_{-9}$	0.129 $^{+6}_{-6}$	0.127 $^{+7}_{-5}$	0.122 $^{+3}_{-3}$
$\kappa_{\text{crit}}$	0.114 $^{+3}_{-3}$	0.112 $^{+8}_{-8}$	0.121 $^{+6}_{-6}$	0.118 $^{+7}_{-5}$	0.113 $^{+3}_{-3}$
$\kappa_s$	0.131 $^{+3}_{-3}$	0.130 $^{+7}_{-8}$	0.140 $^{+6}_{-6}$	0.138 $^{+7}_{-5}$	0.131 $^{+4}_{-4}$

Table 5: Results for the binding energy  $E$  and  $Z^L$  for all smearing types and values of  $\kappa_l$ . Also shown are the extrapolated values at  $\kappa_{\text{crit}}$  and  $\kappa_s$ .

resolved.

Using  $Z_A^{\text{static}} = 0.78$  and  $a^{-1} = 2.9(2)$  GeV we obtain

$$f_B^{\text{static}} = 266 \begin{smallmatrix} +18 \\ -20 \end{smallmatrix} (\text{stat}) \begin{smallmatrix} +28 \\ -27 \end{smallmatrix} (\text{syst}) \text{ MeV} \quad (63)$$

where the systematic error is due to the uncertainty in the lattice scale. Using the value of  $Z^L$  at  $\kappa_s$  we obtain the ratio

$$\frac{f_{B_s}}{f_{B_d}} = 1.16 \begin{smallmatrix} +4 \\ -3 \end{smallmatrix}. \quad (64)$$

We can now compare our findings to other simulations. The direct comparison of  $f_B^{\text{static}}$  [MeV] is however obscured by the different treatment of systematic effects such as the choice of  $Z_A^{\text{static}}$  and the quantity used to set the lattice scale. Therefore we choose to compare the results for  $Z^L$  from simulations using the Wilson action [12, 35, 20, 43, 47, 42] and the  $O(a)$ -improved SW action [36, 44]. Following a suggestion in ref. [48] and assuming a scaling behaviour  $\log Z^L \sim \log a$  and  $g^{-2} \sim \log a$ , we plot  $\log Z^L$  as a function of  $\beta$  in Figure 5. It is seen that the results (with the possible exception of ref. [35]) are well aligned for  $\beta \geq 5.9$ , which supports the argument that scaling occurs in this region of  $\beta$ . Furthermore there is consistency between the results coming from the variational approach ([43, 42] and this work) and those using the conventional approach [47, 36, 44].

The most striking observation is that, as far as  $Z^L$  is concerned, there is practically no difference between the results obtained using the Wilson action and the SW action. A direct comparison was carried out by the APE Collaboration at  $\beta = 6.4$  [44] and  $\beta = 6.0$  [20], and no difference within the statistical errors could be found. At first sight this may not seem surprising, since in the static theory improvement is performed in the light quark sector for which its effects on the mass spectrum were found to be small [14]. However, the renormalisation factor  $Z_A^{\text{static}}$  at leading order in  $\alpha_s$  is quite different for the improved and unimproved action.<sup>5</sup> In fact this difference amounts to an increase of 10–15% in the case of the SW action in the current range of  $\beta$  values. Consequently, collaborations working with the SW action quote relatively high values for  $f_B^{\text{static}}$  in general, compared to those using the usual Wilson action.

We conclude that at present the most severe systematic error in  $f_B^{\text{static}}$  is the uncertainty in the renormalisation factor  $Z_A^{\text{static}}$ . As in the case of the corresponding factors for  $B^0 - \overline{B}^0$  mixing, the perturbative estimate for this constant results in a large correction which signals that higher-order contributions may be important. A non-perturbative determination of  $Z_A^{\text{static}}$  using the method advocated in [33] for both the Wilson and the SW action is therefore of utmost importance.

---

<sup>5</sup>The one-loop expressions for  $Z_A^{\text{static}}$  for the  $O(a)$ -improved theory were computed independently by the authors of [27] and [28].



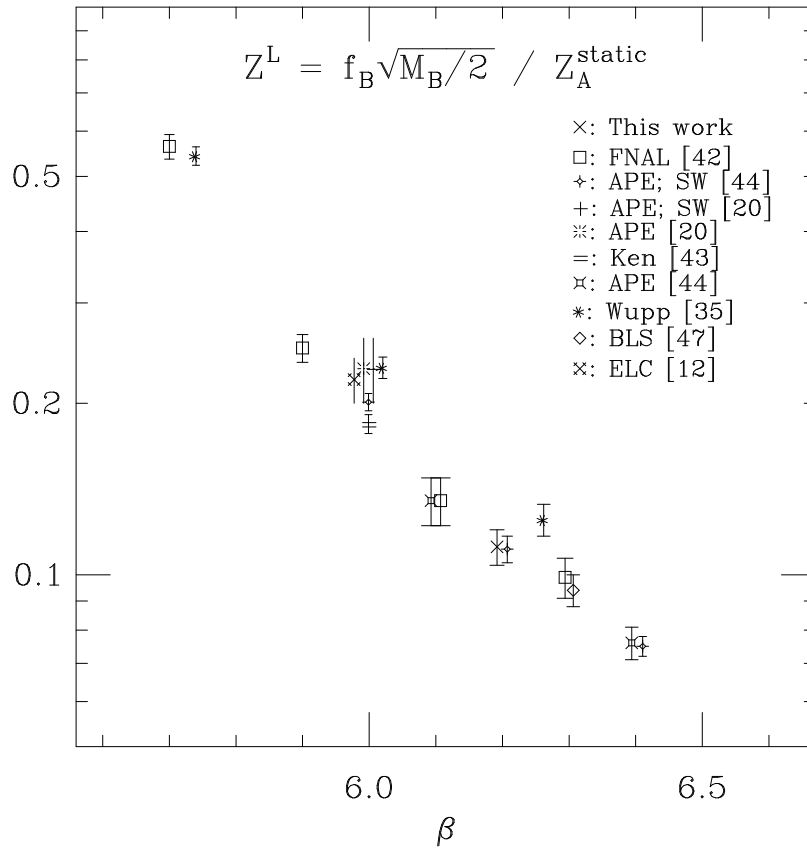


Figure 5:  $Z^L$  plotted logarithmically versus  $\beta$  using data from several simulations obtained using both the Wilson and the SW action.

Systematic errors in  $f_B^{\text{static}}$  coming from uncertainties in the lattice scale will be further reduced once quantities that show good scaling behaviour, such as the 1S-1P splitting in charmonium or the hadronic scale  $R_0$ , become available for a wide range of  $\beta$ .

### 3.5 Phenomenological Implications

We can now combine our best estimates from the previous two subsections into estimates for  $f_B\sqrt{B_B}$ . Using the results in eqs. (54) and (63) we find

$$f_{B_d}\sqrt{B_{B_d}} = 269 \begin{smallmatrix} +18 \\ -25 \end{smallmatrix} (\text{stat}) \begin{smallmatrix} +29 \\ -28 \end{smallmatrix} (\text{syst}) \text{ MeV}. \quad (65)$$

Using the values obtained after extrapolation to the strange quark mass we also quote the phenomenologically interesting ratios

$$\frac{f_{B_s}\sqrt{B_{B_s}}}{f_{B_d}\sqrt{B_{B_d}}} = 1.16 \begin{smallmatrix} +4 \\ -4 \end{smallmatrix} (\text{stat}) \begin{smallmatrix} +2 \\ -1 \end{smallmatrix} (\text{syst}) \quad (66)$$

$$\frac{f_{B_s}^2 B_{B_s}}{f_{B_d}^2 B_{B_d}} = 1.34 \begin{smallmatrix} +9 \\ -8 \end{smallmatrix} (\text{stat}) \begin{smallmatrix} +5 \\ -3 \end{smallmatrix} (\text{syst}) \quad (67)$$

$$\frac{f_{B_s}^2 B_{B_s} M_{B_s}}{f_{B_d}^2 B_{B_d} M_{B_d}} = 1.37 \begin{smallmatrix} +9 \\ -8 \end{smallmatrix} (\text{stat}) \begin{smallmatrix} +5 \\ -4 \end{smallmatrix} (\text{syst}), \quad (68)$$

where the systematic error is obtained from the spread of values using the systematic errors on  $B_{B_d}$ ,  $B_{B_s}$ , as well as the result for  $Z^L$  from a 1-state fit.

The phenomenological implication of our results for  $f_{B_d}$ , eq. (63), or  $f_{B_d}\sqrt{B_{B_d}}$ , eq. (65), is, however, uncertain due to a number of systematic effects such as

- the lack of an extrapolation to the continuum limit
- large uncertainties in the values of the renormalisation constants  $Z_A^{\text{static}}$ ,  $Z_L, \dots, Z_N$
- the need to account for  $O(\Lambda_{\text{QCD}}/m_b)$  corrections
- quenching, i.e. neglecting the effects of quark loops.

In ref. [42] it was shown that the extrapolation of  $f_B^{\text{static}}$  to the continuum can yield a result below 200 MeV (albeit with a fairly large upper uncertainty). We have performed a tentative extrapolation, combining our result with the result of ref. [44]. The extrapolation gave a central value of  $f_B^{\text{static}} \simeq 250$  MeV at zero lattice spacing for the SW action<sup>6</sup>. The difference between the two results is partly due to the fact that  $Z_A^{\text{static}}$  is significantly smaller for the Wilson action than for the SW action as we mentioned before.

---

<sup>6</sup>The extrapolated value does not change if  $R_0$  is used to set the scale instead of the string tension.

Lattice estimates for  $f_B$ , especially in the static approximation, should therefore be treated with caution for phenomenological purposes. However, it is reasonable to assume that systematic effects partly cancel in ratios such as  $f_{B_s}/f_{B_d}$ . In fact, as was shown in [42], the  $a$  dependence of this ratio is compatible with zero. Therefore, in the following we illustrate the effect of our findings on the CKM matrix, using only the ratios in eqs. (66) to (68), which are considered to be less afflicted with systematic effects.

We focus on attempts to constrain the CKM parameters  $\rho$  and  $\eta$  in the standard Wolfenstein parametrisation. The  $B_d^0 - \overline{B}_d^0$  mixing parameter  $x_d$  is given by

$$x_d = \frac{G_F^2 M_W^2}{6\pi^2} \tau_{B_d} f_{B_d}^2 B_{B_d} M_{B_d} \hat{\eta}_{B_d} y_t f_2(y_t) |V_{td}^* V_{tb}|^2 \quad (69)$$

where  $\tau_{B_d}$  is the  $B_d^0$  lifetime,  $\hat{\eta}_{B_d}$  parametrises short-distance QCD corrections, and  $f_2$  is a slowly varying function of  $y_t = m_t^2/M_W^2$ . The current world average for  $x_d$  is [49]

$$x_d = 0.76 \pm 0.06. \quad (70)$$

Mixing in the  $B_s^0 - \overline{B}_s^0$  system can now be exploited in order to place constraints on the ratio  $|V_{ts}|^2/|V_{td}|^2$ :

$$\frac{x_s}{x_d} = \frac{\tau_{B_s}}{\tau_{B_d}} \frac{\hat{\eta}_{B_s}}{\hat{\eta}_{B_d}} \frac{M_{B_s}}{M_{B_d}} \frac{f_{B_s}^2 B_{B_s}}{f_{B_d}^2 B_{B_d}} \frac{|V_{ts}|^2}{|V_{td}|^2}. \quad (71)$$

In this ratio the dependence on the top quark mass is cancelled, and one is left with an expression involving only the CKM matrix elements plus  $SU(3)_{\text{flavour}}$  breaking terms. Assuming  $\hat{\eta}_{B_s} = \hat{\eta}_{B_d}$ , and taking our estimate for  $f_{B_s}^2 B_{B_s} M_{B_s}/f_{B_d}^2 B_{B_d} M_{B_d}$ , we find

$$\frac{x_s}{x_d} = (1.38 \pm 0.17) \frac{|V_{ts}|^2}{|V_{td}|^2}, \quad (72)$$

where we have used  $\tau_{B_d} = 1.53 \pm 0.09$  ps and  $\tau_{B_s} = 1.54 \pm 0.14$  ps. This result is in good agreement with ref. [51] where the proportionality factor is quoted as 1.25.

Using the experimental result for  $x_d$ , we will now infer a value for the mixing parameter  $x_s$ . This requires an estimate for the ratio  $|V_{ts}|^2/|V_{td}|^2$ , which is usually obtained from global fits using the better-known CKM matrix elements as well as experimental data and other theoretical estimates as input. Various analyses of this kind have been presented in [50, 51, 52, 53, 54, 55]. In the standard Wolfenstein parametrisation the ratio  $|V_{td}|^2/|V_{ts}|^2$  reads

$$\frac{|V_{td}|^2}{|V_{ts}|^2} = \lambda^2(1 - 2\rho + \rho^2 + \eta^2) \quad (73)$$

where  $\lambda = |V_{us}| = 0.2205 \pm 0.0018$  [56]. The constraints on the CKM parameters  $\rho$  and  $\eta$  depend crucially on the actual values of  $f_{B_d} \sqrt{B_{B_d}}$  and  $B_K$ .

In a recent study [52], the authors have obtained values for  $\rho$  and  $\eta$  based on choosing  $B_K = 0.8 \pm 0.2$  (which is in agreement with recent lattice data [57]) and on the top quark

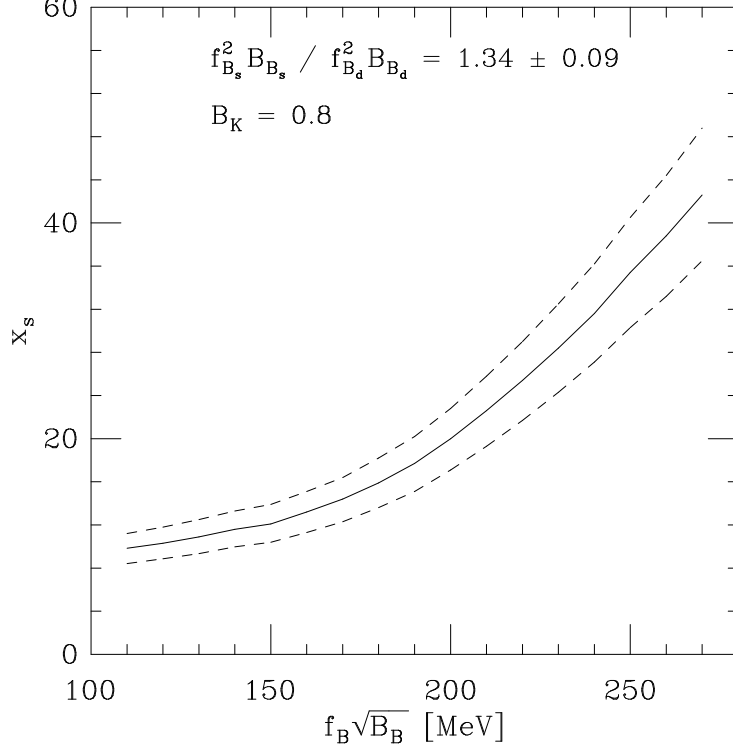


Figure 6: The mixing parameter  $x_s$  as a function of  $f_{B_d} \sqrt{B_{B_d}}$  for a *fixed* value of  $B_K = 0.8$  using our result eq. (68). The solid line follows the central values, whereas the dotted line represents the error band obtained from the errors on  $f_{B_s}^2 B_{B_s} M_{B_s} / f_{B_d}^2 B_{B_d} M_{B_d}$  and  $x_d$ .

mass of  $m_t = 174 \pm 16$  GeV from CDF [58]. Using their values for  $\rho$  and  $\eta$  and our estimate for  $f_{B_s}^2 B_{B_s} M_{B_s} / f_{B_d}^2 B_{B_d} M_{B_d}$  in eq. (68), we plot in Figure 6 the  $B_s^0 - \overline{B}_s^0$  mixing parameter  $x_s$  as a function of  $f_{B_d} \sqrt{B_{B_d}}$ . It is seen that values of  $f_{B_d} \sqrt{B_{B_d}} > 200$  MeV result in practically unmeasurably large values of  $x_s > 20$ . The current experimental lower bound is

$$x_s \geq 9.0 \quad (95\% \text{C.L.}) \quad (74)$$

The error band in the figure is obtained from the errors on our value in eq. (68) and on the experimental result for  $x_d$ . The errors on  $x_s$  should, however, not be taken too seriously, since variations in  $B_K$  introduce large uncertainties in the ratio  $|V_{ts}|^2 / |V_{td}|^2$ .

We conclude this section by noting that the minimum  $\chi^2$  in the global fits in [52] occurs at larger values of  $f_{B_d} \sqrt{B_{B_d}}$  as  $B_K$  is increased. This indicates that large values like  $f_{B_d} \sqrt{B_{B_d}} \geq 200$  MeV, as observed in lattice calculations in the static approximation, favour  $B_K \simeq 1$ . However at present  $B_K$  is not available with good enough accuracy to provide further hints

on the possible range of  $f_{B_d} \sqrt{B_{B_d}}$ .

## 4 Mass Splittings

In this section we report on our results for the  $B_s - B_d$ ,  $\Lambda_b - B$ , and  $B^* - B$  mass splittings. The  $B^* - B$  splitting receives particular attention since it first arises at order  $1/m_Q$  and therefore serves to test the quality of the heavy quark mass expansion. For all the splittings computed we make a comparison with the results using propagating heavy quarks and with experimental data.

### 4.1 The $B_s - B_d$ mass difference

The  $B_s - B_d$  mass splitting is obtained from the chiral behaviour of the binding energy  $E$  extracted from fits to the pseudoscalar 2-point function according to eq. (39) [13]. Assuming a linear dependence of  $E$  on the light quark mass, we fit the chiral behaviour of  $E$  according to

$$E(\kappa) = A + B \frac{1}{2} \left( \frac{1}{\kappa} - \frac{1}{\kappa_{\text{crit}}} \right) \quad (75)$$

such that  $M_{B_s} - M_{B_d}$  is obtained from

$$E(\kappa_s) - E(\kappa_{\text{crit}}) = M_{B_s} - M_{B_d} = B \frac{1}{2} \left( \frac{1}{\kappa_s} - \frac{1}{\kappa_{\text{crit}}} \right). \quad (76)$$

The results for different smearing types, 1-state and 2-state fits, as well as correlated and uncorrelated chiral extrapolations, are shown in Table 4.1.

	EXP		CUB	DCB	INV
$M_{B_s} - M_{B_d}$	1-state	2-state	1-state	1-state	1-state
cor	0.029 $^{+3}_{-4}$	0.030 $^{+5}_{-5}$	0.028 $^{+4}_{-4}$	0.029 $^{+4}_{-4}$	0.029 $^{+3}_{-3}$
unc	0.027 $^{+4}_{-4}$	0.027 $^{+9}_{-7}$	0.028 $^{+5}_{-5}$	0.030 $^{+4}_{-6}$	0.028 $^{+4}_{-3}$

Table 6: The mass difference  $M_{B_s} - M_{B_d}$  in lattice units for all smearing types, using both correlated and uncorrelated fits. For exponential smearing the results from 2-state fits are also shown.

Taking the correlated value of the 2-state fit to the exponentially smeared correlator as our best estimate, and using  $a^{-1} = 2.9(2)$  GeV to convert into physical units we find

$$M_{B_s} - M_{B_d} = 87 \text{ }^{+15}_{-12}(\text{stat}) \text{ }^{+6}_{-12}(\text{syst}) \text{ MeV} \quad (77)$$

where the systematic error combines the spread of values obtained from the uncertainty in  $a^{-1}$  [GeV], using the 1-state result and performing an uncorrelated extrapolation.

This result is in excellent agreement with ref. [42], where a value of  $86 \pm 12 \begin{smallmatrix} +7 \\ -9 \end{smallmatrix}$  MeV is quoted as the continuum result. In a recent high-statistics simulation by the APE Collaboration [44] using the SW action at  $\beta = 6.2$ , the  $M_{B_s} - M_{B_d}$  splitting was quoted as  $58 \pm 14$  MeV. In general, APE's results for a range of  $\beta$  values [44] seem somewhat lower than those reported in [42]. This is partly due to the fact that the string tension was used in [44] to set the lattice scale, giving a lower value (e.g.  $a^{-1} = 2.55$  GeV at  $\beta = 6.2$ ) than we use. Converting APE's result into lattice units, one finds  $aM_{B_s} - aM_{B_d} = 0.023(6)$  which is to be compared to our determination of  $aM_{B_s} - aM_{B_d} = 0.030 \begin{smallmatrix} +5 \\ -5 \end{smallmatrix}$ , and thus the two simulations are not in disagreement. Table 4.1 contains a collection of results in physical units from simulations using the static approximation.

$M_{B_s} - M_{B_d}$ [MeV]	Ref.	Comments
$87 \begin{smallmatrix} +15 & +6 \\ -12 & -12 \end{smallmatrix}$	this work	static, SW, $\beta = 6.2$
$58 \pm 14$	[44]	static, SW, $\beta = 6.2$
$70 \pm 10$	[36]	static, SW, $\beta = 6.2$
$86 \pm 12 \begin{smallmatrix} +7 \\ -9 \end{smallmatrix}$	[42]	static, Wilson, $a = 0$
$71 \pm 13 \begin{smallmatrix} +0 \\ -16 \end{smallmatrix}$	[13]	static, Wilson, $\beta = 6.0$
$96 \pm 6$	[56]	experiment

Table 7: Our value for the  $B_s - B_d$  mass splitting in physical units compared to other simulations using the static approximation. Also shown is the experimental value.

The result in eq. (77) can now be compared to the results using propagating heavy quarks [10]: extrapolating the pseudoscalar mass splitting  $M_{P_s} - M_{P_d}$  linearly in  $1/M_{P_d}$  either to  $M_{P_d} = \infty$  or to  $M_{B_d}$ ,  $M_{D_d}$  one finds

$$M_{B_s} - M_{B_d} = 84 \begin{smallmatrix} +14 & +6 \\ -12 & -6 \end{smallmatrix} \text{ MeV}, \quad M_{P_d} = \infty \quad (78)$$

$$M_{B_s} - M_{B_d} = 93 \begin{smallmatrix} +12 & +6 \\ -12 & -7 \end{smallmatrix} \text{ MeV}, \quad M_{P_d} = M_{B_d} \quad (79)$$

$$M_{D_s} - M_{D_d} = 107 \begin{smallmatrix} +12 & +8 \\ -12 & -6 \end{smallmatrix} \text{ MeV}, \quad M_{P_d} = M_{D_d}. \quad (80)$$

The result at  $M_{B_d} = \infty$  is in excellent agreement with the static result in eq. (77). Furthermore, the value at  $M_{P_d} = M_{B_d}$  agrees very well with the experimental result of  $96 \pm 6$  MeV [56]. The experimental value for  $M_{D_s} - M_{D_d}$  is  $99.1 \pm 0.6$  MeV [56], which is compatible with our estimate.

We conclude that for the  $M_{B_s} - M_{B_d}$  mass splitting it appears possible to interpolate between

the static result and those obtained using propagating heavy quarks. From the behaviour of the splitting with  $1/M_P$  the size of  $\Lambda_{\text{QCD}}/m_Q$  corrections is estimated at around 10% at the mass of the  $B$  meson.

## 4.2 The $\Lambda_b - B$ splitting

In order to study the mass splitting of the  $\Lambda_b$  and the  $B$  meson, we define a smeared interpolating field  $\Lambda_\alpha^S(\vec{x}, t)$  according to

$$\Lambda_\alpha^S(\vec{x}, t) \equiv \epsilon_{ijk} b_\alpha^i(\vec{x}, t) \sum_{\vec{x}'} f(\vec{x}, \vec{x}') \left( u^j(\vec{x}', t) C \gamma_5 d^k(\vec{x}', t) \right) \quad (81)$$

where  $f(\vec{x}', \vec{x})$  is one of the smearing functions in eqs. (13) and (17)–(20), and  $C$  is the charge conjugation matrix. In the above definition the spin of the baryon is carried by the heavy quark field  $b(x)$ .

We define correlators of the  $\Lambda_b$  according to

$$C_{\Lambda_b}^{SS}(t) \equiv \sum_{\vec{x}} \langle \Lambda_\alpha^S(\vec{x}, t) \Lambda_\alpha^{\dagger S}(0) \rangle \xrightarrow{t \gg 0} \left( Z_{\Lambda_b}^S \right)^2 e^{-E_{\Lambda_b} t} \quad (82)$$

$$C_{\Lambda_b}^{LS}(t) \equiv \sum_{\vec{x}} \langle \Lambda_\alpha^L(\vec{x}, t) \Lambda_\alpha^{\dagger S}(0) \rangle \xrightarrow{t \gg 0} Z_{\Lambda_b}^L Z_{\Lambda_b}^S e^{-E_{\Lambda_b} t} \quad (83)$$

where  $S = \text{EXP, CUB, DCB, INV}$ . We then obtain the  $\Lambda_b - B$  mass difference from an exponential fit to the following ratio of smeared-smeared ( $SS$ ) correlators

$$\frac{C_{\Lambda_b}^{SS}(t)}{C^{SS}(t)} \equiv \frac{\sum_{\vec{x}} \langle \Lambda^S(\vec{x}, t) \Lambda^{\dagger S}(0) \rangle}{\sum_{\vec{x}} \langle A_4^S(\vec{x}, t) A_4^{\dagger S}(0) \rangle} \xrightarrow{t \gg 0} \text{const.} \times e^{-(E_{\Lambda_b} - E)t} \quad (84)$$

where

$$E_{\Lambda_b} - E = M_{\Lambda_b} - M_{B_d}. \quad (85)$$

We used the same smearing functions in the numerator and denominator of the ratio in eq. (84), although there is *a priori* no reason why one should do so. However, we found that the uncertainty in the ratio was dominated by the baryon correlator, and therefore we did not expect any gain in trying to optimise the signal using different smearing functions for the mesonic correlator. The ratios defined in eq. (84) gave short but clear plateaux in the range  $9 \leq t \leq 11$ .

The same procedure can of course be applied to the local-smeared ( $LS$ ) correlators  $C_{\Lambda_b}^{LS}(t)$  and  $C^{LS}(t)$ . However, we observed that the effective mass plots for the ratio of  $LS$  correlators do not show clear plateaux. In addition, the fits of the correlators tend to give estimates for the splitting that are higher by up to two standard deviations, which further suggests that the ground state is not completely isolated in  $LS$  correlators.

$M_{\Lambda_b} - M_B$				
$\kappa_l$	EXP	CUB	DCB	INV
0.14144	0.22 $^{+2}_{-2}$	0.23 $^{+2}_{-2}$	0.22 $^{+2}_{-2}$	0.23 $^{+2}_{-2}$
0.14226	0.18 $^{+2}_{-3}$	0.19 $^{+4}_{-3}$	0.18 $^{+3}_{-3}$	0.19 $^{+2}_{-2}$
0.14262	0.16 $^{+3}_{-4}$	0.17 $^{+6}_{-5}$	0.14 $^{+5}_{-6}$	0.16 $^{+3}_{-3}$
$\kappa_{\text{crit}}$	0.14 $^{+3}_{-3}$	0.17 $^{+3}_{-3}$	0.16 $^{+4}_{-3}$	0.16 $^{+3}_{-3}$
$\chi^2/\text{dof}$	0.01	0.18	0.78	1.88

Table 8: The  $\Lambda_b - B$  mass splitting in lattice units at all three values of the light quark mass and extrapolated to the chiral limit.

The ratio of correlators eq. (84) was fitted to a single exponential for  $9 \leq t \leq 11$  at all values of  $\kappa_l$ . In Table 4.2 we list our results in lattice units.

Exponential smearing gave the cleanest signal at all values of  $\kappa_l$ . Assuming a linear dependence on the light quark mass, we extrapolated  $M_{\Lambda_b} - M_B$  to the chiral limit. Again, the results from exponential smearing showed a very good linearity and consequently gave low  $\chi^2/\text{dof}$  in the chiral fits (see Table 4.2). Furthermore, correlated and uncorrelated extrapolations gave almost the same central values. In contrast, the CUB, DCB and INV smearing types gave differing, though statistically consistent, results for correlated and uncorrelated fits. The  $\chi^2/\text{dof}$ 's are, however, larger and fairly high for gauge-invariant smearing.

We therefore take our best estimate from the exponentially smeared correlators. In physical units we obtain

$$M_{\Lambda_b} - M_{B_d} = 420 \text{ }^{+100}_{-90}(\text{stat}) \text{ }^{+30}_{-30}(\text{syst}) \text{ MeV} \quad (86)$$

with the systematic error coming from the uncertainty in  $a^{-1} [\text{GeV}]$ . Our value can be compared to other simulation results and the experimental number in Table 4.2. Comparing with the experimental value, it is seen that our new result is a marked improvement over a previous simulation in the static approximation [13].

In Figure 7 we plot our static result together with recent data obtained with propagating heavy quarks [60, 59]. Our value, compared to an earlier study [13], is in much better agreement with the mass behaviour of the results using propagating heavy quarks. In fact, an extrapolation in  $1/M_P$  of these results to the static limit would be compatible with our value within the (relatively large) statistical errors. For further discussion of the mass behaviour, the reader is referred to [59].



$M_{\Lambda_b} - M_{B_d} [\text{MeV}]$	Ref.	Comments
$420^{+100}_{-90} {}^{+30}_{-30}$	this work	static, SW
$720 \pm 160 {}^{+0}_{-130}$	[13]	static, Wilson
$359^{+55}_{-45} {}^{+27}_{-26}$	[59]	prop., SW
$458 \pm 144 \pm 18$	[60]	prop., Wilson
$362 \pm 50$	[56]	experiment

Table 9: Our value for the  $\Lambda_b - B_d$  mass splitting compared to other simulations using the Wilson action and/or propagating heavy quarks. Also shown is the experimental value.

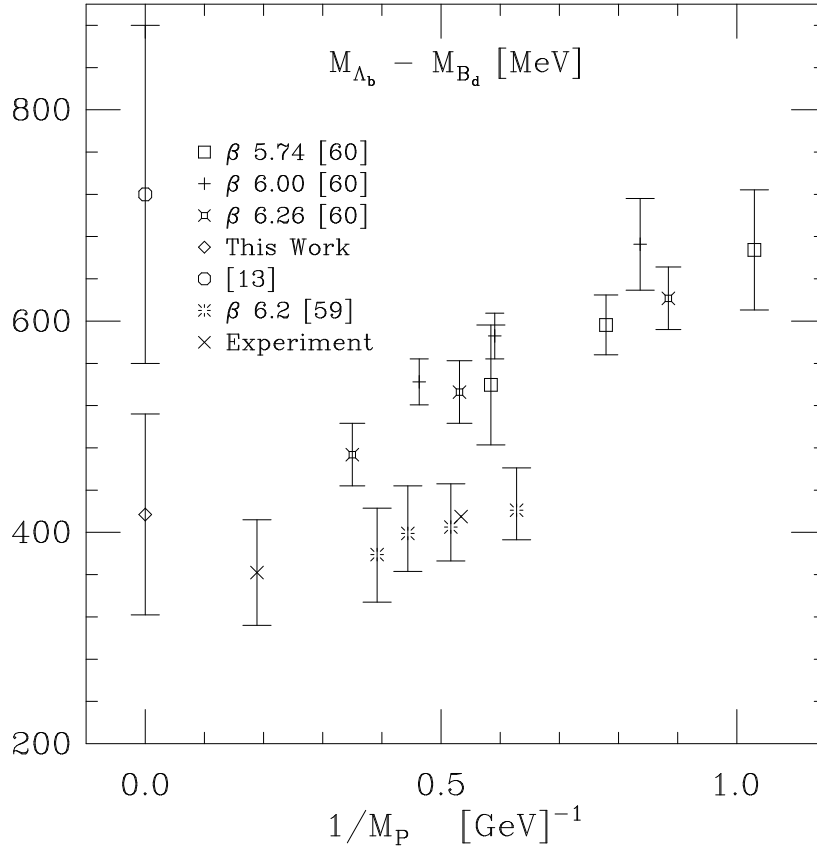


Figure 7: The  $\Lambda_b - B$  splitting in the static approximation (diamonds) compared to other simulations and the experimental values for the  $\Lambda_b - B$  and  $\Lambda_c - D$  splittings. Only statistical errors are shown.

### 4.3 The $B^* - B$ splitting

Within the framework of large mass expansions, the  $B^* - B$  mass splitting plays an important rôle, since it appears at order  $1/m_Q$ ; at lowest order (i.e. in the static approximation)  $M_{B^*} = M_B$ . At order  $1/m_Q$  the splitting arises due to the spin-dependent, chromomagnetic correction term to the quark propagator

$$S_\sigma^1(x, 0) = \frac{1 + \gamma_4}{2} \delta(\vec{x}) \sum_{i < j} \int_0^t d\tau \mathcal{P}_{\vec{x}}(t, \tau) \sigma_{ij} F_{ij}(\vec{x}, \tau) \mathcal{P}_{\vec{0}}(\tau, 0) \quad (87)$$

where  $\mathcal{P}_{\vec{x}}(t, \tau)$  and  $\mathcal{P}_{\vec{0}}(\tau, 0)$  are defined according to eq. (10), and  $F_{ij}$  is a lattice definition of the field tensor.

Following the discussion in [13, 61] we compute the  $B^* - B$  splitting from the insertion of  $S_\sigma^1(x, 0)$  into the correlation function. The usual static correlator is given by

$$C_0(t) \equiv - \sum_{\vec{x}} \langle \gamma_4 \gamma_5 S_Q(x, 0) \gamma_4 \gamma_5 S_l(0, x) \rangle \quad (88)$$

where  $S_Q(x, 0)$  is defined in eq. (9), and  $S_l(x, y)$  is the light quark propagator. In addition, we define

$$C_\sigma(t) \equiv - \sum_{\vec{x}} \langle \gamma_4 \gamma_5 S_\sigma^1(x, 0) \gamma_4 \gamma_5 S_l(0, x) \rangle \quad (89)$$

For large time separations, the ratio  $R_\sigma(t) \equiv C_\sigma(t)/C_0(t)$  shows a linear behaviour

$$R_\sigma(t) \equiv \frac{C_\sigma(t)}{C_0(t)} \xrightarrow{t \gg 0} A_\sigma + B_\sigma t. \quad (90)$$

The splitting  $M_{B^*}^2 - M_B^2$  is then given by the linear slope  $B_\sigma$  according to

$$M_{B^*}^2 - M_B^2 = Z_\sigma \frac{4}{3} B_\sigma. \quad (91)$$

where  $Z_\sigma$  is the renormalisation constant of the magnetic moment operator of the heavy quark [62, 63]. As in the case of the renormalisation constant  $Z_L$  defined in eq. (36), we insert the reduced value of the quark self-energy into the expression given in [63]. Using the “boosted” value of the gauge coupling in the numerical evaluation of  $Z_\sigma$  at one loop, we find [63]

$$Z_\sigma = 1.76. \quad (92)$$

This is a very large correction, which suggests that higher-order contributions are likely to be important and highlights the necessity of a non-perturbative determination of  $Z_\sigma$ .

In our simulation the  $SS$  correlator  $C_\sigma(t)$  was calculated using only gauge-invariant (INV) smearing. In the  $LS$  case, for which more smearing functions were used, the linear behaviour of  $R_\sigma(t)$  could not be established reliably. Thus, we cannot compare different smearing types for the  $B^* - B$  splitting and therefore restrict the discussion to gauge-invariant smearing.

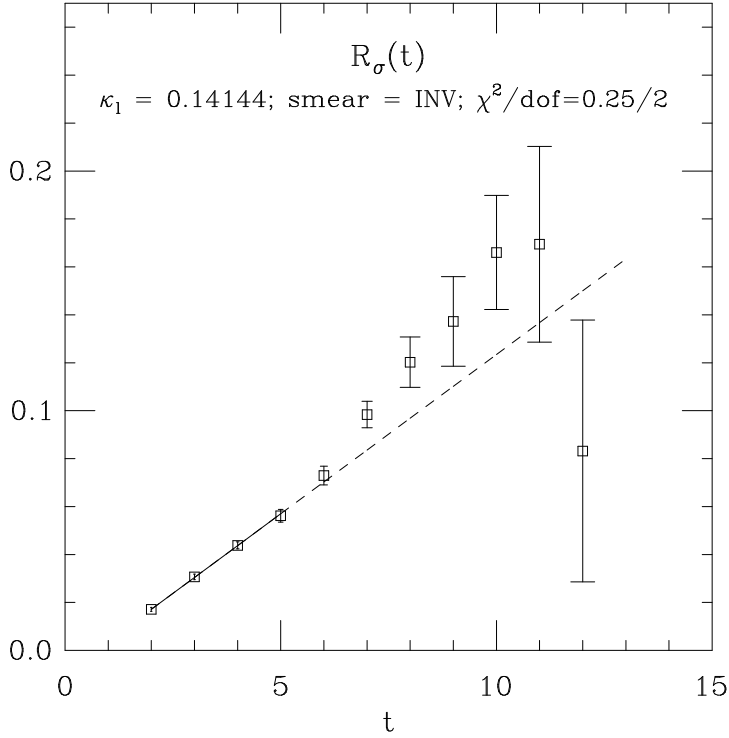


Figure 8: The ratio  $R_\sigma(t)$  for gauge-invariant smearing at  $\kappa_l = 0.14144$ . The fit to eq. (90) is shown as a solid line in the fitting interval  $2 \leq t \leq 5$  and continued as the dotted line for larger times.

The ratio  $R_\sigma(t)$  was fitted to the functional form in eq. (90) for  $2 \leq t \leq 5$  at all three values of  $\kappa_l$ . Figure 8 shows the signal at  $\kappa_l = 0.14144$  together with the fit. It appears that in addition to the linear behaviour of  $R_\sigma(t)$  for very small  $t$ , there is also a linear increase for  $7 \leq t \leq 11$ , albeit with much larger statistical errors. Fits to eq. (90) in this time interval lead to values of  $B_\sigma$  which are larger by up to two standard deviations than those obtained using  $2 \leq t \leq 5$ . The fits at larger times are, however, very sensitive to small variations in the fitting interval. We regard the two-sigma deviation at higher  $t$  as a correlated statistical effect, and believe that the asymptotic behaviour is already observed for small  $t$ . Of course, this must be confirmed in future simulations with higher statistics.

The results for the values of the linear slope parameter  $B_\sigma$  from correlated fits are shown in Table 4.3 together with the linearly extrapolated value at  $\kappa_{\text{crit}}$ . Using uncorrelated fits gives essentially the same results. The values for  $B_\sigma$  increase slightly with decreasing light quark mass, as was already observed in [13], but are also consistent, within the statistical errors,

with  $B_\sigma$  being independent of the light quark mass.

$\kappa_l$	$B_\sigma$
0.14144	0.0133 $^{+7}_{-7}$
0.14226	0.0137 $^{+7}_{-8}$
0.14262	0.0137 $^{+8}_{-8}$
$\kappa_{\text{crit}}$	0.0143 $^{+8}_{-8}$
$\kappa_s$	0.0136 $^{+7}_{-7}$
$\chi^2/\text{dof}$	0.54

Table 10: The fitted linear slope  $B_\sigma$  of the ratio  $R_\sigma(t)$  in lattice units at all values of  $\kappa_l$ , in the chiral limit and at the strange quark mass, extracted from the smeared-smeared (INV) correlator.

Multiplying by  $Z_\sigma 4/3$  and converting into physical units we find

$$M_{B^*}^2 - M_B^2 = 0.281 \begin{smallmatrix} +15 \\ -16 \end{smallmatrix} (\text{stat}) \begin{smallmatrix} +40 \\ -37 \end{smallmatrix} (\text{syst}) \text{ GeV}^2 \quad (93)$$

$$M_{B_s^*}^2 - M_{B_s}^2 = 0.268 \begin{smallmatrix} +13 \\ -13 \end{smallmatrix} (\text{stat}) \begin{smallmatrix} +38 \\ -36 \end{smallmatrix} (\text{syst}) \text{ GeV}^2 \quad (94)$$

with the systematic error coming from the uncertainty in  $a^{-1}$  only. A comparison with experimental data and other simulations is made in Table 4.3. Our result for the  $B^* - B$  splitting is lower than the experimental value by almost a factor of 2. Also, contrary to the experimental observation, our estimate for the  $B_s^* - B_s$  splitting is lower than the one for  $B^* - B$ . This can partly be accounted for by the opposite chiral behaviour of the splitting seen on the lattice. It is interesting to note, however, that both the experimental and lattice determinations of  $M_{B_s^*}^2 - M_{B_s}^2$  yield a result that is compatible within errors with the corresponding value of  $M_{B^*}^2 - M_B^2$ .

The use of the  $O(a)$ -improved SW action for the light quark does not lead to a considerable increase in the splitting, as a comparison with the result of ref. [13] shows. This is not the case for propagating heavy quarks. When the SW action is used for both heavy and light quarks [10], one obtains a value that is also about half of the experimental result. This is still an improvement over the case of propagating heavy Wilson quarks [13] which gives a value about 10 times below the experimental result. As far as the hyperfine splitting is concerned, we therefore conclude that the main benefits of using the  $O(a)$ -improved action are obtained in the case of relativistic heavy quarks. Given the large uncertainty in  $Z_\sigma$ , the Eichten expansion and propagating heavy quarks give comparable results if the SW action is employed. The discrepancy between the lattice and experimental results may, at least partially, be ascribed to quenching effects, as has been argued in ref. [64].

$M_{B^*}^2 - M_B^2 [\text{GeV}^2]$	$M_{B_s^*}^2 - M_{B_s}^2 [\text{GeV}^2]$	Ref.	Comments
$0.281^{+15}_{-16}{}^{+40}_{-37}$	$0.268^{+13}_{-13}{}^{+38}_{-36}$	this work	static, SW
$0.27 \pm 0.05 - 0.07$		[13]	static, Wilson
$0.202^{+76}_{-84}{}^{+29}_{-27}$		[10]	prop., SW
$0.488 \pm 0.006$	$0.508 \pm 0.028$	[56]	experiment

Table 11: Our value for the  $B^* - B$  and  $B_s^* - B_s$  mass splittings compared to other simulations and experiment. The value of  $Z_\sigma$  used in [13] has been evaluated using the reduced value of the quark self-energy and the “boosted” gauge coupling.

## 5 Summary and Conclusions

In this paper we have reported on the results from an extensive study of weak matrix elements and the spectroscopy of heavy quark systems using the static approximation. A large part of our analysis was devoted to studying different types of smeared (extended) operators used in order to improve the signal/noise ratio and the isolation of the ground state. Although exponential or gauge-invariant smearing gave the best signal for most quantities, all the smearing functions gave remarkably consistent results. In addition, the variational approach employed in the determination of  $f_B^{\text{static}}$  demonstrated the compatibility of results obtained using this more refined fitting procedure with those from the usual single-exponential fits. Thus we are confident that we correctly isolate matrix elements and spectroscopy data from the ground state contribution of suitable correlators.

We obtain a good signal for the various four-fermi operators relevant for  $B^0 - \overline{B}^0$  mixing. Our estimate for  $B_B$  in the static approximation is in agreement with its value in the vacuum insertion approximation. Regarding  $f_B$ , we note that our determination of  $Z^L = f_B^{\text{static}} \sqrt{2/M_B/Z_A^{\text{static}}}$  is consistent with other simulations.

Among the systematic errors present in this simulation, the most important (apart from quenching) are due to uncertainties in the renormalisation constants relating the matrix elements on the lattice to their continuum counterparts. These systematic effects manifest themselves most severely in our estimate for the  $B$  parameter, and in the case of  $f_B^{\text{static}}$ , where there is practically no difference in  $Z^L$  for the Wilson and the SW actions, yet the corresponding values of  $Z_A^{\text{static}}$  differ by about 10–15 %. Also, the large value of  $Z_\sigma$  in eq. (92) implies that higher-order contributions may be important in the perturbative evaluation of this constant.

Our results for the  $B_s - B_d$  and  $\Lambda_b - B$  splittings compare very well with experimental estimates, although the statistical errors, especially for the  $\Lambda_b - B$  splitting, are still large.

The  $B^* - B$  splitting obtained from a  $1/m_Q$  correction to the static limit, however, does not agree with experiment. Using the SW action for the light quarks does not lead to a significant increase in the lattice estimate of  $M_{B^*}^2 - M_B^2$ . Future simulations using dynamical quarks may reveal whether the discrepancy between the lattice and experimental results is due to quenching effects.

The static approximation, in conjunction with a refined numerical analysis, remains a valuable tool in lattice studies of heavy quark systems. It plays the crucial rôle of guiding the extrapolation of results obtained using propagating heavy quarks to the mass of the  $b$  quark, by providing direct information at infinite quark mass.

In future, one should concentrate on the analysis of systematic effects such as non-perturbative determinations of the renormalisation constants. In the case of  $B_B$  it would be highly desirable to repeat the calculation for propagating heavy quarks, preferably with an improved fermion action, in order to study the mass dependence.

**Note added:** after completion of this work, we received several papers, [65]–[69], presenting results for the  $B$  parameter [65, 66, 67],  $f_B$  [65, 66, 68, 69], the mass splittings  $M_{B_s} - M_{B_d}$ ,  $M_B - M_{B^*}$  [65],  $B_K$  [66] and discussing phenomenological implications [67]. The conclusions of this paper remain unaltered, though, since the reported numbers are in agreement with our findings.

**Acknowledgements** We thank Guido Martinelli, Vicente Giménez and members of the APE Collaboration for interesting discussions, and, in particular, for alerting us to an error in the calculation of the  $B^* - B$  splitting, as presented in the preprint version of this paper. This research was supported by the UK Science and Engineering Research Council under grants GR/G 32779 and GR/H 49191, by the Particle Physics and Astronomy Research Council under grant GR/J 21347, by the European Union under HCM Network grant CHRX-CT92-0051, by the University of Edinburgh and by Meiko Limited. We thank the Daresbury Rutherford Appleton Laboratories for the use of the Cray Y-MP. We are grateful to Edinburgh University Computing Service for maintaining service on the Meiko i860 Computing Surface and, in particular, to Brian Murdoch for allowing access to a field test multi-processor DEC Alpha machine. JM acknowledges the support of a Foreign and Commonwealth Office Scholarship. CTS (Senior Fellow) and DGR (Advanced Fellow) acknowledge the support of the Particle Physics and Astronomy Research Council.

## References

- [1] M.B. Voloshin and M.A. Shifman, Sov. J. Nucl. Phys. 45 (1987) 292; Sov. J. Nucl. Phys. 47 (1988) 511.
- [2] N. Isgur and M.B. Wise, Phys. Lett. B232 (1989) 113; Phys. Lett. B237 (1990) 527.
- [3] H. Georgi, Phys. Lett. B240 (1990) 447.
- [4] *For recent reviews see:* D. Weingarten, Nucl. Phys. B (Proc. Suppl.) 34 (1994) 29; C.W. Bernard, *ibid.* 47; G. Martinelli, Nucl. Phys. B (Proc. Suppl.) 42 (1995) 127.
- [5] E. Eichten, Nucl. Phys. B (Proc. Suppl.) 4 (1988) 170.
- [6] L. Maiani, G. Martinelli and C.T. Sachrajda, Nucl. Phys. B368 (1992) 281; G. Martinelli and C.T. Sachrajda, Phys. Lett. B354 (1995) 423.
- [7] K. Symanzik, in: *Mathematical Problems in Theoretical Physics*, ed. R. Schrader, R. Seiler and D.A. Uhlenbrock, Springer Lecture Notes in Physics, vol. 153 (1992) 47.
- [8] B. Sheikholeslami and R. Wohlert, Nucl. Phys. B259 (1985) 572.
- [9] G. Heatlie, C.T. Sachrajda, G. Martinelli, C. Pittori and G.C. Rossi, Nucl. Phys. B352 (1991) 266.
- [10] UKQCD Collaboration (R.M. Baxter et al.), Phys. Rev. D49 (1994) 1594.
- [11] APE Collaboration (C.R. Allton et al.) Nucl. Phys. B (Proc. Suppl.) 34 (1994) 456.
- [12] C.R. Allton, C.T. Sachrajda, V. Lubicz, L. Maiani and G. Martinelli, Nucl. Phys. B349 (1991) 598.
- [13] M. Bochicchio, G. Martinelli, C.R. Allton, C.T. Sachrajda and D.B. Carpenter, Nucl. Phys. B372 (1992) 403.
- [14] UKQCD Collaboration (C.R. Allton et al.), Nucl. Phys. B407 (1993) 331.
- [15] UKQCD Collaboration (C.R. Allton et al.), Phys. Rev. D49 (1994) 474.
- [16] Ph. Boucaud, O. Pène, V.J. Hill, C.T. Sachrajda and G. Martinelli, Phys. Lett. B220 (1989) 219; E. Eichten, G. Hockney and H. Thacker, Nucl. Phys. B (Proc. Suppl.) 17 (1990) 529; S. Güsken, *ibid.* 361.
- [17] UKQCD Collaboration (C.R. Allton et al.), Phys. Rev. D47 (1993) 5128.

- [18] M.L. Paciello et al., Phys. Lett. B289 (1992) 405; Phys. Lett. B276 (1992) 163.
- [19] J. Mandula and M. Ogilvie, Phys. Lett. B248 (1990) 156.
- [20] APE Collaboration (C.R. Allton et al.), Nucl. Phys. B413 (1994) 461.
- [21] B. Efron, SIAM Review 21 (1979) 460.
- [22] R. Sommer, Nucl. Phys. B411 (1994) 839.
- [23] UKQCD Collaboration (H. Wittig), Nucl. Phys. B (Proc. Suppl.) 42 (1995) 288.
- [24] UKQCD Collaboration (D.S. Henty et al.), Phys. Rev. D51 (1995) 5323.
- [25] E. Eichten and B. Hill, Phys. Lett. B234 (1990) 511.
- [26] E. Eichten and B. Hill, Phys. Lett. B240 (1990) 193.
- [27] A. Borrelli and C. Pittori, Nucl. Phys. B385 (1992) 502.
- [28] O.F. Hernández and B.R. Hill, Phys. Lett. B289 (1992) 417.
- [29] G.P. Lepage and P.B. Mackenzie, Nucl. Phys. B (Proc. Suppl.) 20 (1992) 173; Phys. Rev. D48 (1992) 2250.
- [30] P.B. Mackenzie, Nucl. Phys. B (Proc. Suppl.) 30 (1993) 35.
- [31] J.M. Flynn, O.F. Hernández and B.R. Hill, Phys. Rev. D43 (1991) 3709.
- [32] V. Giménez, Nucl. Phys. B375 (1992) 582; Nucl. Phys. B401 (1993) 116.
- [33] G. Martinelli, C. Pittori, C.T. Sachrajda, M. Testa and A. Vladikas, Nucl. Phys. B445 (1995) 81.
- [34] E. Eichten, G. Hockney and H. Thacker, Nucl. Phys. B (Proc. Suppl.) 17 (1990) 529.
- [35] C. Alexandrou, S. Güsken, F. Jegerlehner, K. Schilling and R. Sommer, Nucl. Phys. B414 (1994) 815.
- [36] APE Collaboration (C.R. Allton et al.), Phys. Lett. B326 (1994) 295.
- [37] M.B. Gavela et al., Nucl. Phys. B306 (1988) 677.
- [38] D. Seibert, Phys. Rev. D49 (1994) 6240.
- [39] W. Marciano, Phys. Rev. D29 (1984) 580.
- [40] C. Bernard, T. Draper, G. Hockney and A. Soni, Phys. Rev. D38 (1988) 3540.



- [41] A. Abada et al., Nucl. Phys. B376 (1992) 172.
- [42] A. Duncan, E. Eichten, J. Flynn, B. Hill, G. Hockney and H. Thacker, Phys. Rev. D51 (1995) 5101.
- [43] T. Draper and C. McNeile, Nucl. Phys. B (Proc. Suppl.) 34 (1994) 453.
- [44] C.R. Allton et al., Nucl. Phys. B (Proc. Suppl.) 42 (1995) 385.
- [45] G.C. Fox, R. Gupta, O. Martin and S. Otto, Nucl. Phys. B205 (1982) 188;  
M. Lüscher and U. Wolff, Nucl. Phys. B339 (1990) 222;  
A.S. Kronfeld, Nucl. Phys. B (Proc. Suppl.) 17 (1990) 313.
- [46] J. Mehegan, Ph.D. Thesis, University of Edinburgh (1995).
- [47] C.W. Bernard, J.N. Labrenz and A. Soni, Phys. Rev. D49 (1994) 2536.
- [48] C.R. Allton, Nucl. Phys. B437 (1995) 641.
- [49] R. Forty, Proceedings of ICHEP94, Glasgow, July 20 – 27, 1994, ed. P.J. Bussey and I.G. Knowles, IOP Publishing, Bristol (1995) 171.
- [50] M. Lusignoli, L. Maiani, G. Martinelli and L. Reina, Nucl. Phys. B369 (1992) 139.
- [51] A. Ali and D. London, DESY 93-022, to be publ. in Proc. of *ECFA Workshop on the Physics of a B Meson Factory*, ed. R. Aleksan, A. Ali (1993).
- [52] A. Ali and D. London, Z. Phys. C65 (1995) 431.
- [53] J.L. Rosner, in: *B Decays*, 2<sup>nd</sup> Ed., ed. S. Stone, World Scientific, Singapore (1994) 470;  
J.L. Rosner, presented at 2<sup>nd</sup> IFT Workshop on Yukawa Couplings and the Origins of Mass, Gainesville, Florida, 11 – 13 Feb 1994, [hep-ph/9405404](#).
- [54] A. Soni, Proceedings of ICHEP94, Glasgow, 20 – 27 July 1994, ed. P.J. Bussey and I.G. Knowles, IOP Publishing, Bristol (1995) 709.
- [55] M. Ciuchini, E. Franco, G. Martinelli and L. Reina, ROME-1091-1995, [hep-ph/9503277](#).
- [56] Particle Data Group (L. Montanet et al.), Phys. Rev. D50 (1994) 1173.
- [57] R. Gupta, D. Daniel, G. Kilcup, A. Patel and S.R. Sharpe, Phys. Rev. D47 (1993) 5113;  
S.R. Sharpe, Nucl. Phys. B (Proc. Suppl.) 34 (1994) 403.
- [58] F. Abe et al. (CDF Collaboration), Phys. Rev. Lett. 73 (1994) 225; Phys. Rev. D50 (1994) 2966.

- [59] UKQCD Collaboration (K.C. Bowler et al.), Edinburgh Preprint 95/555, [hep-lat/9601022](#)
- [60] C. Alexandrou et al., Phys. Lett. [B337](#) (1994) 340.
- [61] UKQCD Collaboration (A.K. Ewing), Nucl. Phys. B (Proc. Suppl.) [42](#) (1995) 331.
- [62] E. Eichten and B.R. Hill, Phys. Lett. [B243](#) (1990) 427.
- [63] J.M. Flynn and B.R. Hill, Phys. Lett. [B264](#) (1991) 173.
- [64] UKQCD Collaboration (C.R. Allton et al.), Phys. Lett. [B292](#) (1992) 408;  
A. El-Khadra, Nucl. Phys. B (Proc. Suppl.) [30](#) (1993) 449.
- [65] T. Draper and C. McNeile, presented at International Symposium on Lattice Field Theory, Melbourne, Australia, 11 – 15 July 1995, [hep-lat/9509060](#).
- [66] JLQCD Collaboration (S. Aoki et al.), presented at International Symposium on Lattice Field Theory, Melbourne, Australia, 11 – 15 July 1995, [hep-lat/9510033](#).
- [67] A. Soni, presented at International Symposium on Lattice Field Theory, Melbourne, Australia, 11 – 15 July 1995, [hep-lat/9510036](#).
- [68] MILC Collaboration (C. Bernard et al.), presented at International Symposium on Lattice Field Theory, Melbourne, Australia, 11 – 15 July 1995, [hep-lat/9509045](#).
- [69] C.R. Allton, presented at International Symposium on Lattice Field Theory, Melbourne, Australia, 11 – 15 July 1995, [hep-lat/9509084](#).